

# **Computational Modeling of Skeletal Muscle Adaptation to Changes in Physical Activity**

---

A Thesis

Presented to  
the faculty of the School of Engineering and Applied Science  
University of Virginia

---

in partial fulfillment  
of the requirements for the degree

Master of Science

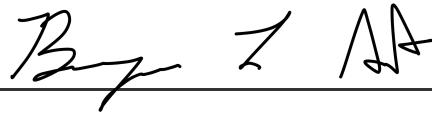
by

Benjamin L Anton

August 2019

# APPROVAL SHEET

This Thesis  
is submitted in partial fulfillment of the requirements  
for the degree of  
Master of Science

Author Signature: 

This Thesis has been read and approved by the examining committee:

Advisor: Silvia S. Blemker

Committee Member: Shayn Peirce-Cottler

Committee Member: Joseph Hart

Committee Member: \_\_\_\_\_

Committee Member: \_\_\_\_\_

Committee Member: \_\_\_\_\_

Accepted for the School of Engineering and Applied Science:



Craig H. Benson, School of Engineering and Applied Science

August 2019

UNIVERSITY OF VIRGINIA

**Computational Modeling of Skeletal Muscle  
Adaptation to Changes in Physical Activity**

A THESIS

SUBMITTED TO THE GRADUATE SCHOOL  
IN PARTIAL FULLFILLMENT OF THE REQUIREMENTS

for the degree

MASTER OF SCIENCE

Field of Biomedical Engineering

By

**Benjamin L. Anton**

CHARLOTTESVILLE, VIRGINIA

August 2019

# ABSTRACT

## COMPUTATIONAL MODELING OF SKELETAL MUSCLE ADAPTATION TO CHANGES IN PHYSICAL ACTIVITY

**Benjamin L. Anton**

The scientific community has long sought to understand the relationship between muscle adaptation and physical activity through numerous experimentations from the tissue level to the subcellular level. Mechanical overuse results in increases in muscle size (hypertrophy) while disuse results in decreases in muscle size (atrophy). One hope is that by expanding our understanding at the cellular level we will be able to improve muscle hypertrophy or mitigate atrophy for patients in populations such as sports medicine, recreational conditioning, and bed rest patients. Computational modeling provides the opportunity to compile the vast number of individual experimental observations into a comprehensive framework with the ability to predict observed outcomes. There is a need for novel computational modeling frameworks that can predict human skeletal muscle adaptations to various states of activity and can treat each muscle cell type independently. This study seeks to advance our theoretical understanding of this relationship by compiling experimental data on muscle adaptation, postulating an activity-based differential equation that reflects macro insights on the cellular scale, integrating the differential equation into a computational framework, and validating empirically-derived parameters that can accurately predict muscle adaptation to various physical activities. Additionally, a novel relationship between fiber recruitment and exercise intensity was constructed by analyzing protein accretion rates by exercise intensity. These parameters were then used to simulate the effect of eight weeks of bed-rest and eight weeks of RE on muscle fiber area.

By analyzing atrophy and hypertrophy simulations, we confirmed that fiber adaptation to physical activity could be accurately represented by three parameters: protein synthesis per nuclei per day ( $\beta_s$ ), the rate of protein degradation per fiber CSA ( $\beta_d$ ), and the number of myonuclei per fiber CSA. Additionally, simulations of muscle adaptation across 29 muscle groups revealed that muscle architecture can be an accurate predictor of muscle atrophy and hypertrophy. Percentages of fiber types I, IIA, and IIB were significantly correlated with normalized hypertrophy ( $R^2 = 0.66$ ,  $p < 0.05$  for all). The strongest predictor of muscle hypertrophy included fiber type distributions as well as initial CSA ( $R^2 = 0.90$ ,  $p < 0.05$ ). Initial fiber CSA of all fiber types were significantly correlated with muscle atrophy (Type I:  $R^2 = 0.28$ ,  $p = 0.003$ ; Type IIA:  $R^2 = 0.33$ ,  $p = 0.001$ ; Type IIB:  $R^2 = 0.33$ ,  $p = 0.001$ ). Simulations also revealed that muscle hypertrophy was significantly correlated to muscle atrophy ( $R^2 = 0.9318$ ,  $p < 0.001$ ), indicating that muscle groups were more prone to either atrophy or hypertrophy based on their architecture. Simulations of detraining and subsequent retraining support the theory of muscle memory, myonuclei retained during periods of disuse enable muscle to quickly adapt to increases in physical activity, by accurately predicting muscle atrophy upon a period of detraining and subsequent hypertrophy upon retraining.

## ACKNOWLEDGEMENTS

These past few years have been a time of great growth and maturity for me. I have learned so much about myself, about the research process, modeling, muscles, presenting, and most importantly, about how to ask the right questions and always keep my head up when things aren't always going the way I would like them to. I would not have been able to learn and grow in the ways that I did without the incredible group of people surrounding me, teaching and supporting me. You all have been huge influences on my life during my graduate career and have helped me become the person I am today.

I would first like to thank my advisor, Dr. Silvia Blemker, for your incredible mentorship throughout this process. Your knowledge of skeletal muscle physiology, computational modeling, and your enthusiasm for learning were invaluable for me. I knew that I could always count on you to ask the questions I would never have thought to ask, and to give me an enthusiastic boost when I needed it. You have taught me so much about skeletal muscle, the modeling process, and scientific research, but more importantly, you have taught me to always remain inquisitive and upbeat. Learning is fun and I cannot think of a person who enjoys learning as much as you do. Thank you, Silvia.

I would also like to thank my Master's committee: Dr. Shayn Peirce-Cottler and Dr. Joseph Hart. Shayn, you have taught me so much about computational modeling and agent-based modeling in particular. I very much enjoyed taking your computational modeling class. I learned so much from that class and from meeting with you to ask questions about my research. Joe, thank you so much for everything you have done for me these past few years. From taking your clinical biomechanics course in my first semester at UVA to working with you and your lab on my first research project at UVA, the muscle volume-torque project, to discussing the clinical relevance of the work I was doing, your mentorship has greatly helped me in everything I have collaborated with you on and has taught me the importance of viewing any problem from multiple angles. I have always firmly believed in finding clinical relevance in all the work I do and your experience and knowledge in this department have helped me greatly when narrowing the scope of my thesis and thinking of the right questions to answer.

In addition, I would like to thank my colleagues for their constant support and advice. Thank you, Kelly Virgilio and Dr. Kyle Martin, for teaching me about ABMs, muscle adaptation, and for providing the research upon which I could build my thesis. Thank you, Dr. Katie Pelland, for always providing me the motivation to keep working and the knowledge that there is always light at the end of the tunnel, even if it takes longer than you anticipated to get there. Thank you, Vi Tran, Adrienne Williams, Dr. Brian Jones, and Hunter Wallace, for always being there when I had questions and for always offering to help me. I am also grateful to Dr. Xiao Hu, Katie Knaus, Evan Terrell, Amanda Meppelink-Westman, Emily Miller, Matt Disalvo, and Ridhi Sahani for being an incredible support structure for me, offering me feedback on my work and presentations, and for making M3 such an incredible lab to be in.

Finally, I would like to thank my family and friends for always being there for me, supporting me when I needed it, and helping me through the many challenges I have faced these past few years. Thank you, Mom, Dad, Rob, Kristi, Ruby, and all the friends I have made at UVA and in Charlottesville. You have made these past few years unforgettable, have always helped me grow, and have always helped me remain enthusiastic and optimistic.

## Table of Contents

1	Introduction .....	1
2	Background and Significance .....	3
2.1	Skeletal Muscle Architecture .....	3
2.2	Skeletal Muscle Adaptation to Disuse .....	7
2.3	Skeletal Muscle Adaptation to Resistance Exercise .....	11
2.4	Significance of the Study .....	14
3	Methods .....	15
3.1	Theoretical Relationship Between Protein Metabolism and Physical Activity .....	15
3.2	Model Design .....	17
3.3	Parameter Estimation .....	23
3.4	Simulations of Muscle Adaptation Across A Range of Muscle Groups.....	30
3.5	Simulations of Muscle Adaptation Following Detraining and Subsequent Retraining .	30
4	Results .....	31
4.1	Model Parameters.....	32
4.2	Muscle Architecture Determines Muscle Adaptation .....	36
4.3	Model Simulations of Detraining and Retraining Support Theory of Muscle Memory	42
5	Discussion.....	44
5.1	Summary and Implications.....	44
5.2	Assumptions and Limitations.....	46
5.3	Contributions and Future Work .....	48
6	References .....	51
7	Appendix .....	56
7.1	Model Acronyms and Terms.....	56
7.2	Netlogo Code, Version 6.0.1 .....	57

## Table of Figures

Figure 2.1 Structure of Muscle .....	4
Figure 2.2 Muscle Memory Theory .....	10
Figure 3.1 Agent-based Model .....	18
Figure 3.2 Flowchart of ABM .....	21
Figure 3.3 Parameter Estimation.....	24
Figure 3.4 Simulated Protein Metabolism During Physical Activity .....	26
Figure 3.5 Estimation of Fiber Recruitment .....	28
Figure 3.6 Estimation of Fiber Recruitment .....	29
Figure 4.1 Atrophy Parameter Validation.....	33
Figure 4.2 Hypertrophy Parameter Validation.....	35
Figure 4.3 Euclidean Shortest Distance Dendrogram.....	37
Figure 4.4 Correlation Between Simulated Hypertrophy and Atrophy .....	38
Figure 4.5 Muscle Architecture Can Predict Hypertrophy .....	40
Figure 4.6 Muscle Architecture Can Predict Atrophy .....	41
Figure 4.7 Simulations of Detraining and Retraining.....	43

# 1 Introduction

The scientific community has long sought to understand the relationship between skeletal muscle adaptation and physical activity through numerous studies that measure adaptation at scales ranging from the whole joint to the tissue level to the subcellular level (for example: Ferrando et al., 1966; LeBlanc et al., 1992; Biolo et al., 1995; Berg et al., 1997; Phillips et al., 1997; Bamman et al., 1998; Green et al., 1998; Ohira et al., 1999; Bodine et al., 2001; Campos et al., 2002; Biolo et al., 2004; Fry, 2004; Jackman & Kandarian, 2004; Sandri, 2008; Bruusgaard et al., 2012; Pederson & Febbraio, 2012; Damas et al., 2015; Wisdom et al., 2015). While these experiments have revealed the robust adaptive capacity of muscle, these data have yet to be combined in order to build a fundamental, theoretical understanding of the relationship between different physical activities and muscle fiber size or cross-sectional area (CSA). Skeletal muscle is a highly plastic organ that allows the body to adapt to various physical demands and is an important regulator of human health. Mechanical overuse results in increases in muscle size (hypertrophy) while disuse results in decreases in muscle size (atrophy). I believe that developing a theoretical understanding of muscle at the cellular level will provide new insights that lead to improved treatments for diseases and injuries associated with muscle atrophy, including muscular dystrophy, sarcopenia, and cachexia.

Computational modeling provides the opportunity to compile the vast number of individual experimental observations into a comprehensive framework that has the ability to predict observed outcomes. Through this framework, we can better understand how alterations at the cellular level elicit tissue-wide changes, thereby improving our mechanistic knowledge of how muscle adapts to physical activity. This study seeks to advance our theoretical understanding of this relationship by compiling experimental data on muscle adaptation,



postulating an activity-based differential equation that reflects macro insights on the cellular scale, and validating empirically-derived parameters that can accurately predict muscle adaptation to various physical activities.

Within this computational framework, agent-based modeling is advantageous because it has the ability to prescribe the postulated activity-based differential equation to each muscle fiber and allow each fiber to adapt independently. Previous agent-based models have accurately predicted rat and mouse skeletal muscle adaptations to disuse as well in disease states (Martin et al., 2015; Virgilio et al., 2015; Martin et al., 2016). However, there is yet a computational model that predicts *human* skeletal muscle adaptation to various states of activity.

This thesis describes how a theoretical relationship between skeletal muscle size and changes in physical activity was constructed using a computational framework. Chapter 2 describes an overview of skeletal muscle architecture, how it adapts to changes in activity, and the significance of this study. Chapter 3 describes the theoretical and computational methods employed to describe this relationship. Chapter 4 presents our results, including determined model parameters and results of our simulations. Chapter 5 describes the significance of this study, its limitations, and future directions.

## **2 Background and Significance**

This chapter outlines pertinent background information relevant to this study, including skeletal muscle architecture, the different fiber types and their functions, the mechanisms by which fiber size decreases through disuse atrophy, and the mechanisms by which fiber size is increased during hypertrophy from resistance exercise. Further, this chapter will discuss the significance of this study, the current frameworks that describe skeletal muscle architectural changes, and how this study fills in missing gaps in the understanding of the relationship between changes in muscle size and physical activity.

### **2.1 Skeletal Muscle Architecture**

To properly explain how skeletal muscle adapts its size to physical activity, it is imperative to first consider muscle structure. As observed in Figure 1.1, muscle is a highly organized, hierarchical structure consisting of repeated units added in parallel and in series. The primary cell in skeletal muscle is the muscle fiber—multinucleated cells that are responsible for muscle's ability to contract. When bundled, fibers form muscle fascicles which group to form the whole muscle. Fibers contract by shortening individual contractile units: sarcomeres. These units consist of two major proteins: myosin and actin. When activated, these protein units overlap, shortening the sarcomere. This is the basic mechanism allowing skeletal muscle to shorten and produce movement. Sarcomeres are arranged in parallel and in series to form myofibrils. The increase in the number of myofibrils in a muscle fiber (hypertrophy) enables the fiber to produce a greater amount of contractile force. Conversely, when myofibrils are removed (atrophy), the fibers lose their potential force output.

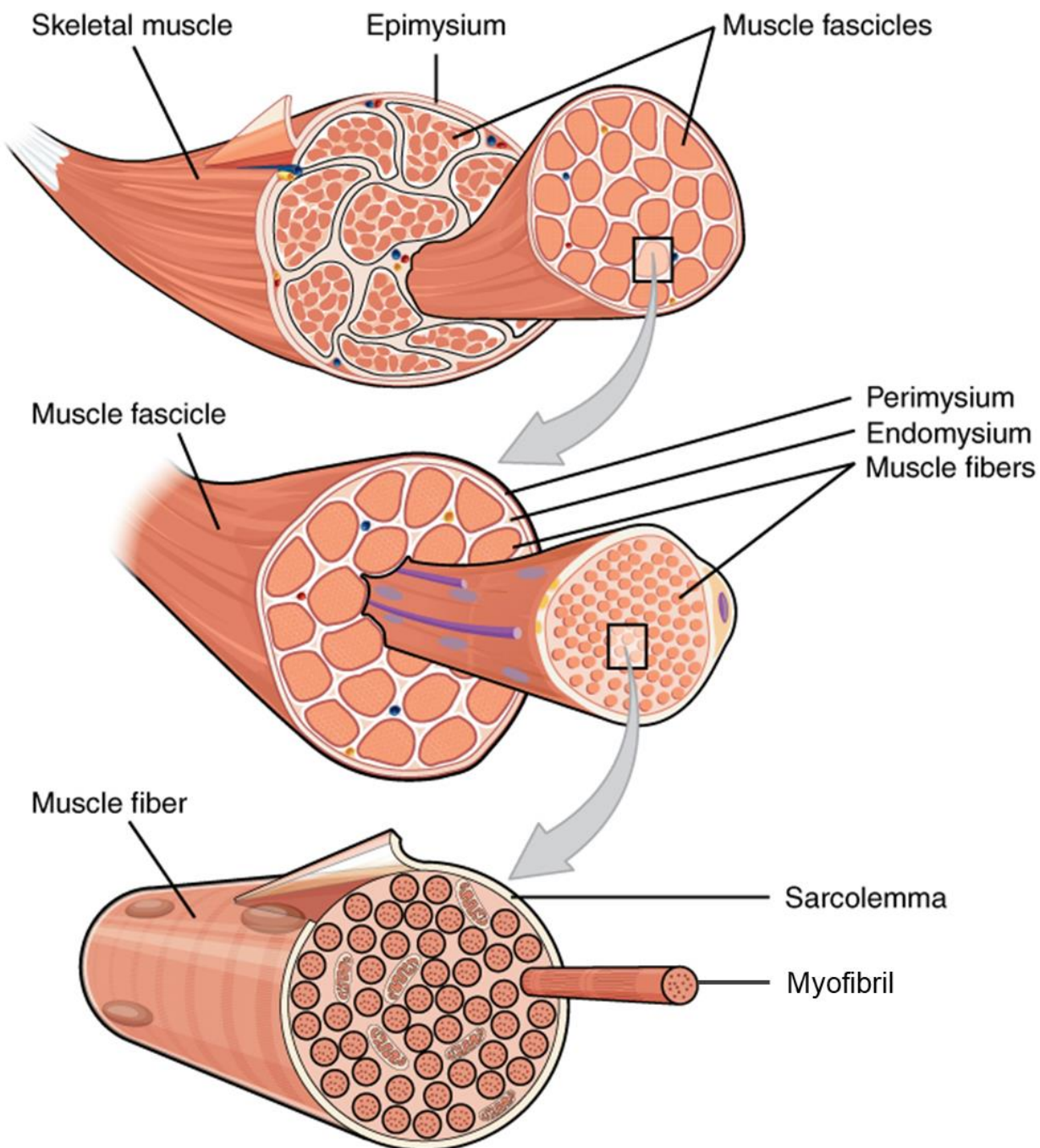


### Figure 2.1 Structure of Muscle

Skeletal muscle is organized in a hierarchical structure consisting of highly organized, repeating structures from the subcellular level to the tissue level. The muscle fiber is the cellular unit of muscle tissue. Fibers are multinucleated and consist of myofibrils added in parallel and in series. Muscle fibers are bundled together to form the muscle fascicle which group to form the muscle body. Skeletal muscle size is regulated by adding (hypertrophy) or removing (atrophy) myofibrils. Figure adapted from OpenStax Anatomy and Physiology 2016.

Skeletal muscle consists of multiple fiber types that are classified into three main groups: Type I, Type IIA, and Type IIB based on mATPase activity, myosin heavy chain form, or biochemical metabolism (Scott et al., 2001). These different fiber types are responsible for allowing muscle to function in a variety of tasks from high endurance activities such as long distance running or posture to high-force output tasks such as lifting heavy objects or rapid propulsion during jumping or sprinting. Type I fibers are responsible for low force, high endurance activities, and rely on oxidative phosphorylation. By contrast, Type IIB fibers are responsible for high force, low endurance activities, and rely on glycolysis. Type IIA fibers are a middle ground between the two fiber types and can perform higher force output than Type I fibers while being more fatigue-resistant than Type IIB fibers. Type IIA fibers function through a mixture of oxidative phosphorylation and glycolysis. These fiber types are distributed differently across different muscle groups in the body according to the muscle's primary function. Additionally, each fiber type adapts differently to various physical activities, allowing the body to perform a variety of tasks while being as metabolically efficient as possible by only increasing the size of fibers that are consistently being used.

**Table 2.1 Muscle Fiber Types and Their Physiological Properties**

	<b>Type I</b>	<b>Type IIA</b>	<b>Type IIB</b>
<b>Twitch Speed</b>	Slow	Fast	Fast
<b>Fatigability</b>	Low	Low	High
<b>Force Output</b>	Low	Intermediate	High
<b>Metabolism</b>	Oxidative Phosphorylation	Oxidative Phosphorylation /Glycolysis	Glycolysis

Fibers are organized in functional groups called motor units, consisting of an alpha motor neuron that sends electrical signals from the central nervous system to the muscle, and all the fibers that neuron innervates (Scott et al., 2001). Motor units are classified by their twitch speed and their fatigability. Generally, there are three types of motor units: Slow Oxidative (SO), Fast Oxidative/ Glycolytic (FOG), and Fast Glycolytic (FG) (Scott et al., 2001). It has been observed that smaller motor units are generally SO and largely comprised of slow-twitch fibers (Type I) whereas larger motor units are generally FOG or FG units and are largely comprised of fast-twitch fibers (Type IIA and IIB) (McPhedran et al., 1965a, 1965b).

As previously mentioned, fiber size is regulated by adding or removing myofibrils through protein metabolism—the balance between protein synthesis and degradation. Protein synthesis is regulated by transcription in the nucleus of a cell (myonuclei). Muscle fibers are by far the largest cells in the body, requiring multiple myonuclei per cell to upkeep protein metabolism. Therefore, it has been theorized that each myonuclei is responsible for regulating a finite volume, termed myonuclear domain (MND) (Cheek et al., 1971; Cheek, 1985). In fiber cross-sections, fibers have an average MND of  $2000 \mu\text{m}^2$  per nuclei (Petrella et al., 2006). However, this domain size has been observed to be correlated to fiber size with larger fibers exhibiting larger domain sizes (Karlsen et al., 2015). The number of myonuclei in a fiber is regulated by removing nuclei through apoptosis, or by adding additional nuclei through myonuclear addition.

Myonuclear addition is the process by which new myonuclei are added to muscle fibers. This process is regulated by one of the other main cell types in muscle tissue: satellite cells. Satellite cells are myonuclei precursor cells nomenclated for their residence between the fiber's

cellular membrane and the basal lamina. Myonuclear addition occurs when quiescent satellite cells imbedded in the basement membrane of fibers are activated to due mechanical or metabolic strain (Chargé & Rudnicki, 2004; Tidball, 2005; Petrella et al., 2006; Petrella et al., 2008).

Satellite cells then proliferate and fuse with muscle fibers. The importance of myonuclear addition will be more fully explained in detail in section 2.3 describing skeletal muscle adaptation to resistance exercise.

## **2.2 Skeletal Muscle Adaptation to Disuse**

Skeletal muscle atrophy is the process by which fiber size is decreased. Disuse atrophy triggered by a loss or decrease in mechanical stimulation is a common problem for bed rest or limb immobilization populations and can result in debilitating muscle weakness. During disuse atrophy, protein metabolism in muscle fibers is altered, resulting in a chronic net loss of contractile proteins. This net loss results in the removal of myofibrils in muscle fibers, causing the fiber's size, and potential force output, to decrease. Protein synthesis has been observed to be the most dynamic variable and is highly influenced by changes in activity. During disuse atrophy, protein synthesis decreases significantly (Ferrando et al., 1996; Paddon & Jones, 2006; Biolo et al., 2004). Furthermore, protein degradation during disuse atrophy has been observed to either not change or fall accordingly with atrophy (Ferrando et al., 1996; Paddon & Jones, 2006).

Decreases in fiber size due to disuse atrophy are largest earlier on (1-30 days) and are seen to plateau after around 90-120 days (Adams et al., 2003). This plateau makes theoretical and logical sense as muscle tissue cannot continue losing size indefinitely. Eventually, protein degradation will decline, with decreasing fiber size, until the protein metabolism in muscle fibers reaches equilibrium—no net gain or loss of contractile protein. This intrinsic mechanism is a built-in negative feedback loop, ensuring that there will always be at least some minimal amount

of muscle tissue. Through experimental observation alone, it would be extremely difficult to determine what this minimum fiber size would be. However, through computational modeling, we could gain a theoretical estimation that should be dependent upon the rate of protein synthesis as well as the rate of protein degradation.

Another important element to track during disuse atrophy is how the number of myonuclei per fiber changes, as the number of myonuclei in muscle fibers is proportional to the amount of protein that can be synthesized. Previous theories proposed that during muscle atrophy, myonuclei in the fibers are removed through apoptosis in order to improve metabolic efficiency (Allen et al., 1999; Gundersen et al., 2016). This theory however has recently been refuted. Through new imaging and labeling techniques to identify myonuclei from other cellular muscle in muscle tissue, experimental observations of myonuclear number in vivo during atrophy has shown there is no significant decrease in myonuclei during prolonged periods of muscle atrophy (Bruusgaard et al., 2012; Ohira et al., 1999; Kadi et al., 2004). These observations have been defined as a new “muscle memory” theory where muscle fibers record a history of physical activity through maintaining their myonuclei (see Figure 2.1). Through retaining myonuclei, fibers retain their capacity to respond quickly to future increases in mechanical demand.

Even though many studies over the years have provided vast experimental data in the attempt to determine how skeletal muscle atrophies, there are still many unanswered mechanistical questions that need to be answered. How can all these individual experimental studies be compiled and analyzed to gain a better understanding of muscle atrophy at multiple scales: tissue-level, cellular-level, subcellular-level? A novel framework that can account for muscle changes at each of these different scales and can effectively analyze and integrate the

experimental observations previously mentioned in this section is needed. However, this new framework must be simple, flexible enough to be easily interpreted and adapted when necessary to fit the needs of other patient populations (sarcopenia, cachexia, etc.), but still be powerful enough to accurately replicate experimental observations of muscle atrophy. In addition, this framework must be able to answer why there are discrepancies in the amount muscle fibers atrophy between different experimental subjects and studies, what determines the degree to which a muscle fiber will atrophy, and be able to predict how fibers with vastly different architectures (fiber type and size) will atrophy. I believe that my computational model described in this thesis can effectively fulfill each of these requirements and provide a more complete understanding of muscular atrophy at multiple scales.



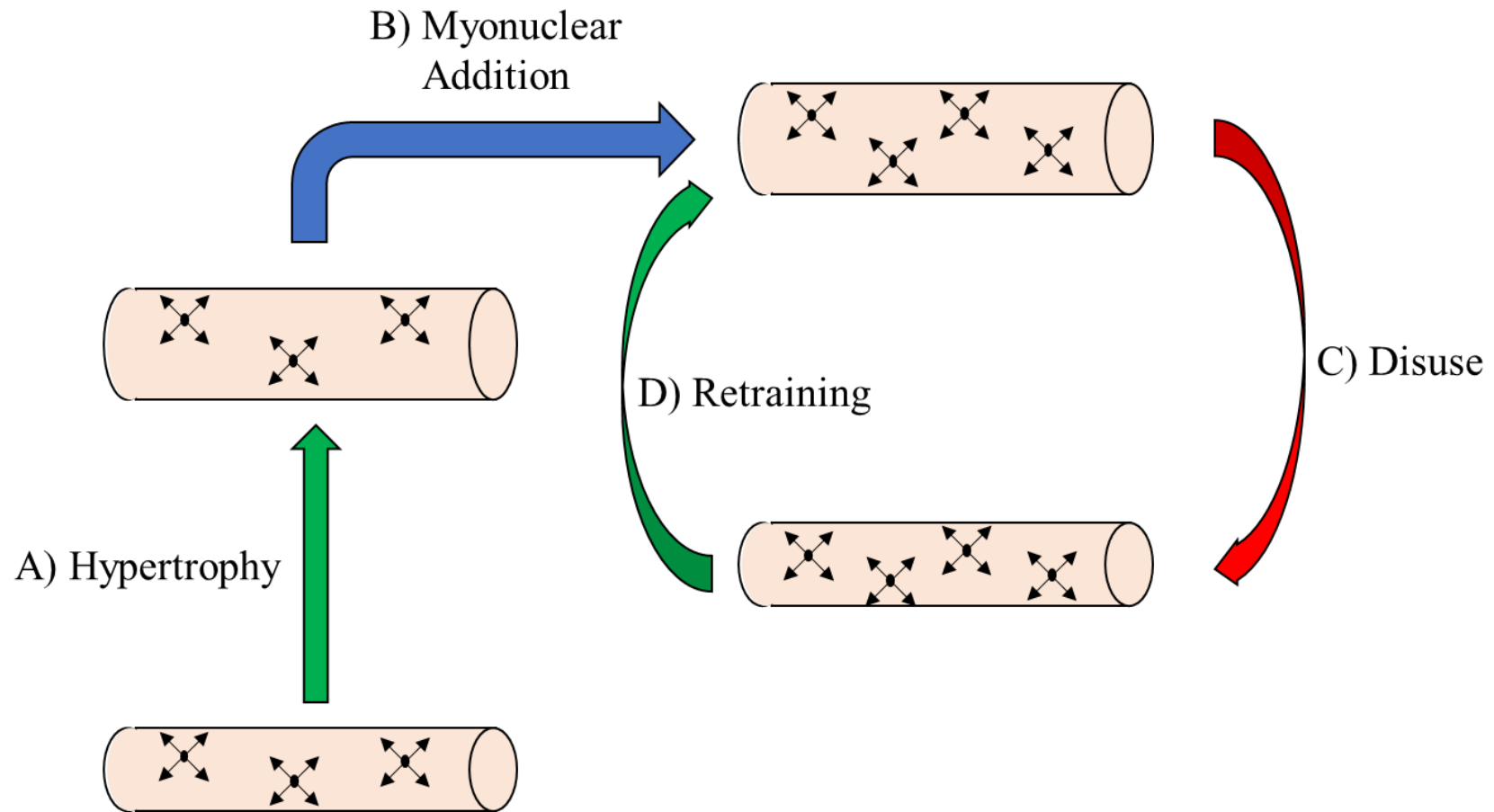


### Figure 2.2 Muscle Memory Theory

Muscle memory theory in which myonuclei are retained in muscle fiber even after atrophy during de-training. A) Positive net protein deposition due to increased physical activity causes the muscle fiber to hypertrophy. B) As the myonuclear domain size increases beyond its MND ceiling of roughly  $2000 \mu\text{m}^2/\text{nuclei}$ , myonuclei are added to the fiber. C) During fiber atrophy because of physical disuse, fiber size decreases. However, myonuclei obtained during initial growth remain in fiber. D) Retained myonuclei allow the muscle fiber to quickly adapt to periods of retraining. Figure adapted from Bruusgaard et al., 2009.

## 2.3 Skeletal Muscle Adaptation to Resistance Exercise

Skeletal muscle has the ability to adapt to increases in physical activity, which will be termed resistance exercise (RE), by enlarging its fibers' sizes (hypertrophy). Through increasing its fibers' size, the whole muscle improves its ability to output force and cope with more demanding activity. In order for fibers to grow in size in response to increased activity, there must be a chronic net deposition of contractile proteins. To a single bout of RE, it has been observed that protein synthesis increases 100% in the fed state while degradation increases 40% (Phillips et al., 1997; Biolo et al., 1995). Again, as with muscle atrophy, it should be noted that protein synthesis is what exhibits the greatest change when physical activity is altered. These protein metabolism elevations are observed across all fiber types if they are recruited and exercised until fatigued, enabling muscle fibers to repair fiber damage and increase fiber CSA (Burd et al., 2010). However, these increases in protein metabolism are only transient. For untrained populations, upregulated protein synthesis and degradation after only a single bout of RE is seen to decrease by 1/3 each 24 hours (Damas et al., 2015). Therefore, in order to produce chronic net protein deposition, sustained multiple bouts of exercise are required.

However, as with muscular atrophy, there must be some internal mechanism inhibiting muscle hypertrophy if muscle is exercised too often to the point that it is overused. This mechanism can be seen in the transient increase in protein degradation following a bout of RE. For a single bout of RE, this upregulated degradation rate is essential for remodeling muscle tissue. Old myofibrils that are damaged need to be broken down so that new myofibrils can be added, strengthening the fibers against future high intensity activity. However, if muscle is overused, protein degradation can increase until it exceeds the fiber myonuclei's protein synthesis. If this happens, muscle will be continuously broken down as it will not have the time

necessary to rebuild itself. Therefore, there is an importance balance between exercising muscle to elicit architectural changes, and exercising the muscle too much to the extent that the muscle fibers are only being broken down. This balance must be accounted for in any theoretical relationship describing how skeletal muscle adapts to increased physical activity.

However, muscle fibers can only adapt to increases in physical activity if they are recruited during RE by their alpha motor neuron. As mentioned previously, the three fiber types differ in regard to their force output and fatigability (see table 1). This allows the body to perform various physical activities efficiently. It has been proposed that motor units are recruited from small to large in order to fulfill the requirements of the task at hand (Henneman et al., 1957, 1956a, 1956b). For example, by recruiting smaller motor units first, muscles can perform precise actions such as picking up delicate objects efficiently. Physiologically, it was determined that smaller motor units are recruited before larger units because their smaller diameters result in lower recruitment thresholds (Bawa et al., 1984). Further studies have supported this theory by demonstrating that recruitment threshold is correlated with the twitch force of recruited motor unit (Riek & Bawa, 1992; Stephens & Usherwood, 1977). Additionally, fatigue index and threshold force have been shown to be inversely correlated—high fatigue index ratings indicate low threshold force: motor units that are fatigue-resistant have low recruitment thresholds (Stephens & Usherwood, 1997). Similar correlations have been shown between contraction strength, percent maximum voluntary contraction (%MVC), and fatigue index (Stephens & Usherwood, 1997). It can therefore be inferred that muscle fibers are generally recruited in order from Type I > Type IIA > Type IIB. However, there is still no theory quantifying fiber recruitment as a function of RE intensity, making any estimation of fiber recruitment difficult.

Once a muscle fiber is recruited and starts to hypertrophy, it is imperative to determine how its myonuclear number and the MND adapt, as the number of myonuclei affects the amount of protein that fiber can produce. As previously stated, the myonuclear domain theory postulates that each myonuclei is responsible for a finite cytoplasmic volume. In other words, myonuclei have a synthesis capacity—they are only able to increase their protein synthesis to an extent. Therefore, they can only upkeep a finite cytoplasmic volume. Muscle fibers' ability to increase protein synthesis up to their capacity is demonstrated in experimental studies where fibers exhibit moderate hypertrophy without myonuclear addition (Kadi et al., 2004; Petrella et al., 2006). However, as fibers continue growing, the existing myonuclei will be unable to sustain the hypertrophy and new myonuclei will need to be recruited. As previously mentioned, the average resting MND has been estimated in muscle fiber cross sections to be around  $2000 \mu\text{m}^2/\text{nuclei}$ , giving insight into a theoretical ceiling that, once reached, would require new myonuclei to be added through myonuclear addition (see Figure 2.1). The theoretical mechanism limiting indefinite myonuclear addition and subsequent fiber hypertrophy is currently unknown. However, it is possible to gain an estimated maximum number of myonuclei per cross section of around 4-5 by studying muscle fibers of bodybuilders (MacDougall et al., 1984; Karlsen et al., 2015). As noted previously, these recruited myonuclei are retained in the fibers, providing a history of physical activity and enabling muscle to respond quickly after periods of detraining and subsequent retraining.

Analyzing these observations has allowed us to gain insight into what mechanisms of skeletal muscle hypertrophy are still unknown: 1) What determines the extent of hypertrophy? 2) How does muscle fiber architecture (fiber type and size) affect muscle growth? 3) How does retaining myonuclei during atrophy allow muscle to hypertrophy quickly after retaining?

Through compiling and analyzing this data, the proposed computational model effectively probed these questions, and was able to suggest novel mechanistic hypothesis regarding muscle growth and retraining.

## 2.4 Significance of the Study

While there are vast amount of experimental data describing how muscle adapts to physical activity, which presents an excellent opportunity to create a comprehensive theoretical framework based on these data. Computational modeling provides the opportunity to compile these individual experimental observations into a comprehensive framework with the ability to predict observed outcomes. This thesis seeks to advance the theoretical understanding of this relationship by compiling experimental data on muscle adaptation, postulating an activity-based differential equation that reflects macro insights on the cellular scale, and validating empirically-derived parameters that can accurately predict muscle adaptation to various physical activities.

Within this computational framework, agent-based modeling is powerful approach because it has the ability to prescribe the postulated activity-based differential equation to each muscle fiber and allow each fiber to adapt independently. Previous agent-based models have accurately predicted rat and mouse skeletal muscle adaptations to disuse as well in disease states (Martin et al., 2015; Virgilio et al., 2015; Martin et al., 2016). However, there is yet a computational model that predicts *human* skeletal muscle adaptation to various states of activity. The goal of this study therefore was to develop an agent-based computational model of human skeletal muscle that will accurately predict experimental observations of skeletal muscle adaptation to changes in activity.

### 3 Methods

This chapter outlines the key elements of the computational framework describing the relationship between fiber size and physical activity. It starts by describing how the theoretical relationship was developed, discussing each term used to describe how physical activity is translated to changes in fiber CSA. This chapter then describes how this theoretical relationship was integrated into a computational modeling framework, including how the model was designed, equations used in the model to simulate how variables in the CSA equations are changed in response to various physical activities (Table 3.1), and how model parameters were determined. Finally, this chapter outlines how the model simulated the response of 22 lower limb muscle groups to one 30-day RE regime.

#### 3.1 Theoretical Relationship Between Protein Metabolism and Physical Activity

To create a novel theoretical relationship describing alterations in fiber size to changes in activity, it is imperative to understand which biomechanical and biological cues influence fiber size. It has been proposed that protein content directly determines fiber size (Phillips et al., 2009; Edgerton et al., 1991). By assuming that protein density is constant within muscle fibers, a relatively simple mathematical relationship between protein metabolism and changes in fiber cross-sectional area (CSA) can be proposed (see Equation 1). In this framework, changes in fiber CSA are directly influenced by fibers' protein metabolism—the balance between protein synthesis and degradation. If the protein synthesis is greater than the protein degradation, the fiber would hypertrophy. Conversely, if the protein degradation is greater than the protein synthesis, the fiber would atrophy. Martin et al., 2015 previously postulated this relationship in the form of a differential equation defining changes in fiber CSA during atrophy. However, this

framework is specific only to cases of muscle atrophy and does not account for the influence that myonuclei have on fiber CSA. Therefore, here we propose a refined differential equation to describe how protein metabolism in a single muscle fiber alters its CSA in all cases of fiber adaptation:

$$\text{Equation 1: } \frac{d\text{CSA}}{dt} = \beta_s * \text{nuclei} - \beta_d * \text{CSA}$$

$$\text{Equation 2: } \text{CSA}_{\infty} = \frac{\beta_s * \text{nuclei}}{\beta_d}$$

As previously described in Chapter 2, the total amount of protein a fiber produces is a function of the number of myonuclei in that fiber cross-section (nuclei) and the rate of protein production in each nuclei ( $\beta_s$ ). Therefore, protein synthesis was modeled as a product of these two variables (Edgerton et al., 1991; Gundersen et al., 2016).  $\beta_s$  is defined as the protein synthesis rate per myonuclei per time ( $\mu\text{m}^2/\text{nuclei}/\text{day}$ ) while the nuclei variable is defined as the number of myonuclei per fiber cross section. Protein degradation was defined as the rate of protein turnover and is regulated by fiber size—larger fibers have higher protein turnover rates (Edgerton et al., 1991). Fiber protein degradation was therefore defined as the product of a protein degradation rate per unit time  $\beta_d$  ( $\text{day}^{-1}$ ) with the fibers CSA ( $\mu\text{m}^2$ ).

$\beta_s$ , nuclei, and  $\beta_d$  were to be altered to describe how a fiber's protein metabolism was modulated by activity. During disuse atrophy,  $\beta_s$  and  $\beta_d$  decreased until they reached defined baseline values—see Section 3.3: Parameter estimation for how baseline values were determined. The number of myonuclei was also kept constant as there have been no observed significant decreases in myonuclei count during disuse atrophy (Bruusgaard et al., 2012; Ohira et al., 1999; Kadi et al., 2004). During daily activity and RE,  $\beta_s$ , and  $\beta_d$  were increased in order to simulate fiber size adaptation observed (Harber et al., 2004). During RE,  $\beta_s$  was increased until a maximum rate was reached, representing each myonuclei's capacity to increase its protein

synthesis in order to adapt to changes in activity (Kadi et al., 2004; Petrella et al., 2006). However, once this capacity was reached, the number of myonuclei per muscle fiber was increased to sustain growth.

Equation 1 describes how fiber CSA changes over time as a function of protein metabolism. As time goes on, muscle atrophy and hypertrophy plateaus (Wisdom et al., 2015). These phenomena were replicated by restricting each fibers'  $\beta_s$ ,  $\beta_d$ , and nuclei variables. As time goes to infinity, the solution to  $CSA(t)$  approaches its theoretical maximum during hypertrophy and its theoretical minimum during atrophy. By taking the limit of  $CSA(t)$  as time goes to infinity ( $CSA_\infty$ )—Equation 2—the theoretical maximum and minimum CSAs were shown to be dependent upon three variables: the number of myonuclei per fiber (nuclei), how much protein each nucleus is synthesizing ( $\beta_s$ ), and the rate at which protein is degraded ( $\beta_d$ ).

### 3.2 Model Design

The equations described in the previous section were integrated into a computational framework to model how muscle fibers adapt to changes in physical activity. An agent-based model (ABM) consisting of 225 fibers was generated to represent a cross section of a skeletal muscle fascicle (Figure 3.1). Human skeletal muscle was modeled to reflect the abundance of experimental evidence prescribing how human muscle adapts to changes in activity (as outlined in Chapter 2). The three major fiber types were included in the model: Type I, Type IIA, and Type IIB. A timestep of one day was used in order to reduce computational cost as well as be able to model individual bouts of resistance exercise and daily changes in fiber protein metabolism. The model was built using Netlogo 6.0.1 and simulation data was organized and analyzed using Matlab R2018a.



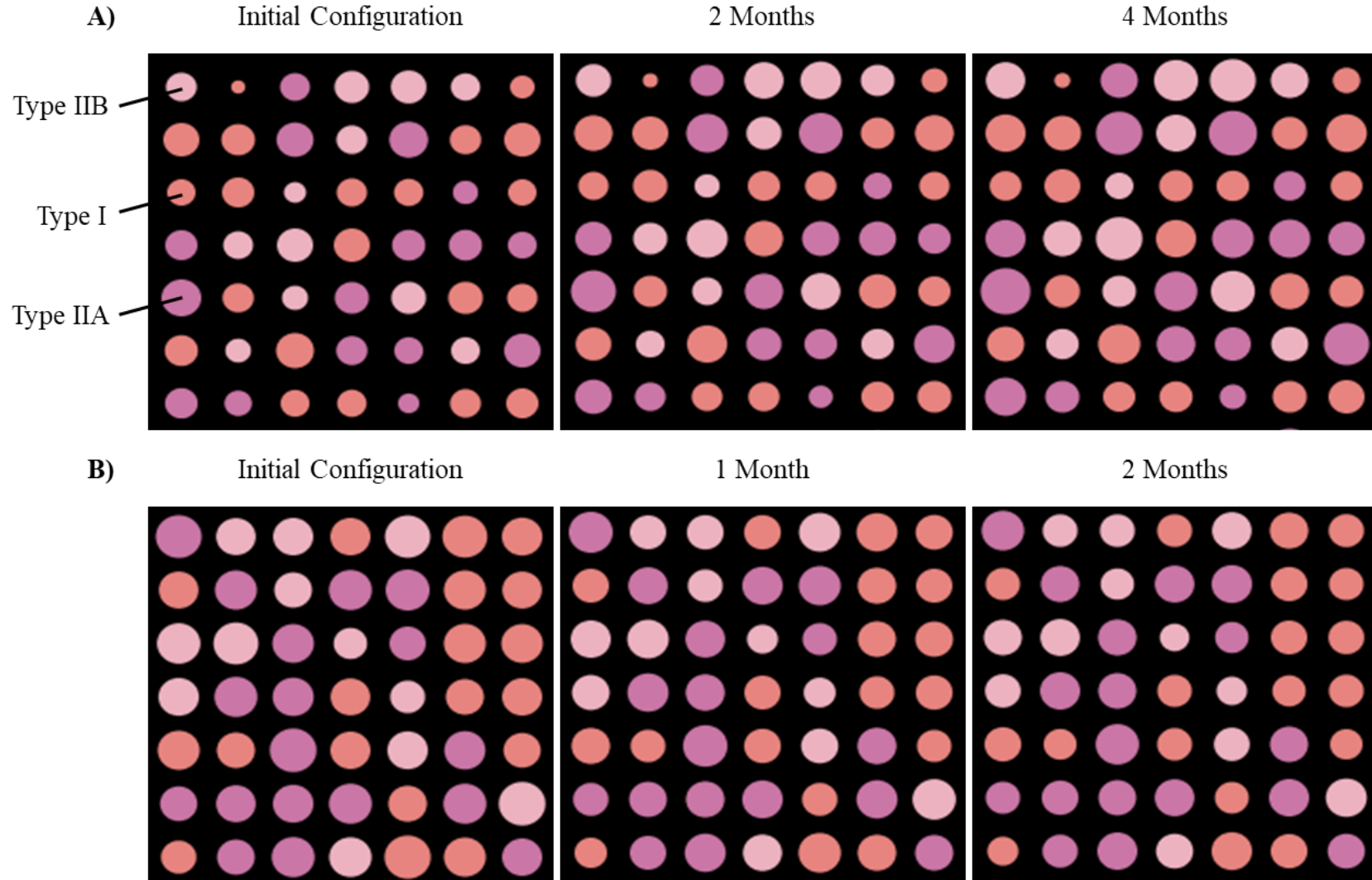


**Figure 3.1 Agent-based Model**

Agent-based model (ABM) of skeletal muscle adaptation. Fiber types I, IIA, and IIB are labelled. A) Muscle fiber hypertrophy due to increased physical activity. B) Muscle fiber atrophy as a result of disuse.

Each fiber was represented as an independent agent and adapted to changes in physical activity according to observed experimental data outlined in Chapter 2 (see Table 3.1 for equations prescribed to fibers). Each muscle fiber could hypertrophy and atrophy independently by tracking their own fiber synthesis, degradation, and myonuclei count. Fiber synthesis and degradation coefficients were designated with minimum baseline values corresponding to bed-rest atrophy. Fiber synthesis, degradation, and nuclei number were designated with maximum values in order to limit fiber growth.

Muscle architecture was initialized by randomly assigning a fiber type and initial CSA based on user-defined inputs. Each fiber was then assigned an initial synthesis coefficient ( $\beta_s$ ), and degradation coefficient ( $\beta_d$ ). The values for these coefficients were tuned to replicate bed-rest atrophy studies and represented baseline synthesis and degradation rates (see Section 3.2: Parameter Estimation). These coefficients were increased with daily activity and resistance exercise. Additionally, the initial number of nuclei for each fiber cross-section was designated using a MND of  $2000 \mu\text{m}^2/\text{nuclei}$  (Karlsen et al., 2015). As myonuclei are distributed throughout the fiber in three dimensions, the nuclei variable for each fiber was a non-integer variable representing the net effect of protein production from the nuclei surrounding that fiber's cross-section. Nuclei that are farther away from the slice would have a lower contribution to that fiber cross-section than nuclei that are closer. Therefore, the model used a continuous (rather than discrete) nuclei variable to approximate the effect of distance from the nuclei to the fiber cross-section.

Once the muscle architecture was initialized, the model entered the fiber routine. First, it would assess what physical activity the fibers experienced: bed rest, daily activity, or resistance exercise—defined by user-inputs (see figure 3.2). If the fibers were assigned bed rest, protein

metabolism would decline if not at baseline values, and the fiber CSA would be adapted.

Otherwise, if the model was set to daily activity or exercise, the model moderately increased the fibers' metabolism according to daily activity. Then, if the model was set to exercise, it would determine if the fibers were exercising that day based on a user-defined input of the number of days of rest between RE routines. If the fibers were exercising, the probability they were recruited was determined as a linear function of exercise intensity (%MVC) (Equations 9-11).

The model would then increase the protein metabolism in the fiber that were recruited. After the fiber routine, the model determined whether myonuclei should be added to the fibers. If the model was set to exercise for 14-days and if the fibers' MND was larger than  $2000\mu\text{m}^2$ , the model recalculated that fiber's myonuclei number (Snijers et al., 2016; Petrella et al., 2006; Petrella et al., 2008; Karlsen et al., 2015). Finally, the model would then repeat the fiber and myonuclei routines until the end of the defined timeframe—where the simulation terminates.

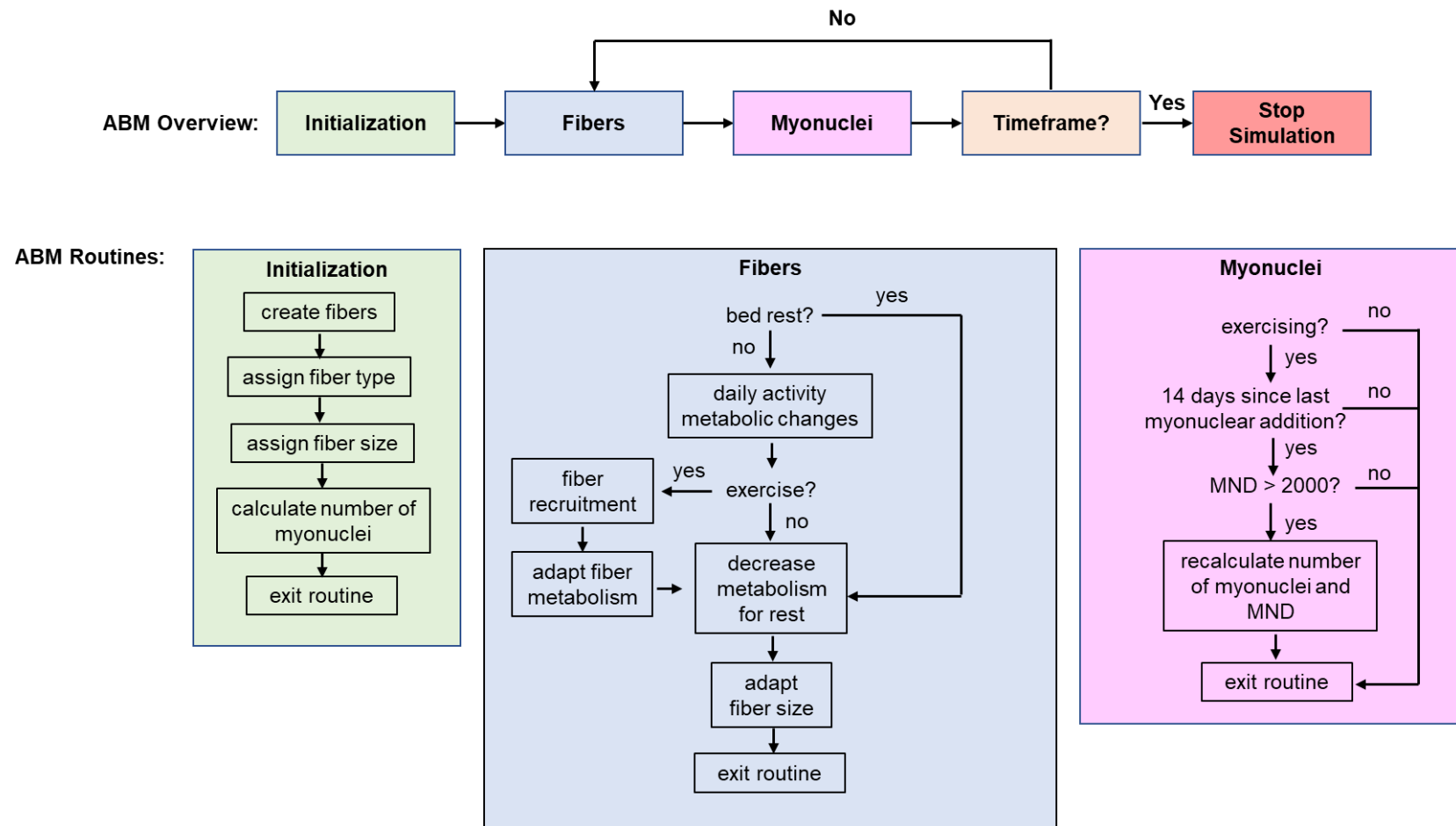


**Figure 3.2 Flowchart of ABM**

Muscle architecture is initialized by assigning a type and size to each fiber agent by means of user-defined inputs. The model then calculates the number of myonuclei in each fiber using a MND of  $2000 \mu\text{m}^2/\text{nuclei}$ . Once initialized, the model assesses what physical activity each fiber will experience: bed rest vs. normal daily activity vs. exercise. The model then adjusts each agents' metabolism and calculates its new size. After the fiber routine, the model determines whether myonuclei should be added. If a fiber's MND is larger than  $2000 \mu\text{m}^2/\text{nuclei}$ , the model recalculates its myonuclei number. The model then repeats the fiber and myonuclei routines until the end of the defined timeframe—when the simulation terminates.

**Table 3.1 Equations Implemented in Model**

Equation Number	Equation as implemented in model
<i>Fiber Adaptation</i>	Euler method was used for solving protein balance between synthesis and degradation.
E1	$CSA_{new} = CSA + \beta_s * nuclei * timestep - \beta_d * CSA * timestep$
E2	$CSA_{\infty} = \beta_s * nuclei / \beta_d$
<i>Daily Activity</i>	Small increases in fiber protein synthesis and degradation with daily activity.
E2	If Type I fiber, $\beta_s = \beta_s + 0.18 * \beta_s$ $\beta_d = \beta_d + 0.06 * \beta_d$
E3	If Type IIA fiber, $\beta_s = \beta_s + 0.1 * \beta_s$ $\beta_d = \beta_d + 0.06 * \beta_d$
E4	If Type IIB fiber, $\beta_s = \beta_s + 0.13 * \beta_s$ $\beta_d = \beta_d + 0.05 * \beta_d$
<i>Exercise</i>	Increases in protein synthesis and degradation with a single bout of RE.
E5	$\beta_s = \beta_s + 1.0 * \beta_s$
E6	If $\beta_d$ is larger than maximum $\beta_d$ , $\beta_s = \beta_{s \max}$
E7	$\beta_d = \beta_d + 0.4 * \beta_d$
E8	If $\beta_d$ is larger than maximum $\beta_d$ , $\beta_d = \beta_{d \max}$
<i>Fiber Recruitment</i>	Chance a fiber is recruited during exercise was calculated as linear function of RE intensity (R = % Chance recruited, I = Exercise intensity or % MVC).
E9	If Type I fiber, $R = 0.0096 * I + 0.1458$
E10	If Type IIA fiber, $R = 0.0106 * I + 0.0543$
E11	If Type IIB fiber, $R = 0.0125 * I - 0.109$
<i>Rest</i>	Fiber protein synthesis and degradation rates were decreased during rest.
E12	$\beta_s = \beta_s - (\beta_s - \beta_{s \text{ baseline}}) / 3$
E13	$\beta_d = \beta_d - (\beta_d - \beta_{d \text{ baseline}}) / 3$

### 3.3 Parameter Estimation

*Determining synthesis and degradation coefficients for bed rest atrophy.*

Synthesis and degradation coefficients for bed rest atrophy were estimated by tuning these parameters such that simulated changes in mean CSA matched those observed experimentally (Berg et al., 1997). Initial mean fiber CSA of the model fibers was prescribed according fiber area measurements reported in Berg et al., 1997. I ran simulations for all fiber types (Type I, IIA, and IIB) for 37 days using a range of degradation ( $\beta_d$ ) ( $2.4\text{—}2.8 \times 10^{-3} \text{ day}^{-1}$ ) and synthesis coefficients ( $\beta_s$ ) ( $35\text{—}50 \mu\text{m}^2/\text{nuclei}^{-1} * \text{day}^{-1}$ ) until the percent error between simulated and experimental fiber areas was  $< 1\%$  (see Figure 3.3). The coefficients,  $\beta_s$  and  $\beta_d$ , were then validated using independent bed rest atrophy studies (Bamman et al., 1998; Widrick et al., 1997). Acceptable rates produced final mean CSA values within the mean and standard deviations observed in these studies. Validated synthesis and degradation coefficients were then used as baseline rates in all future simulations.

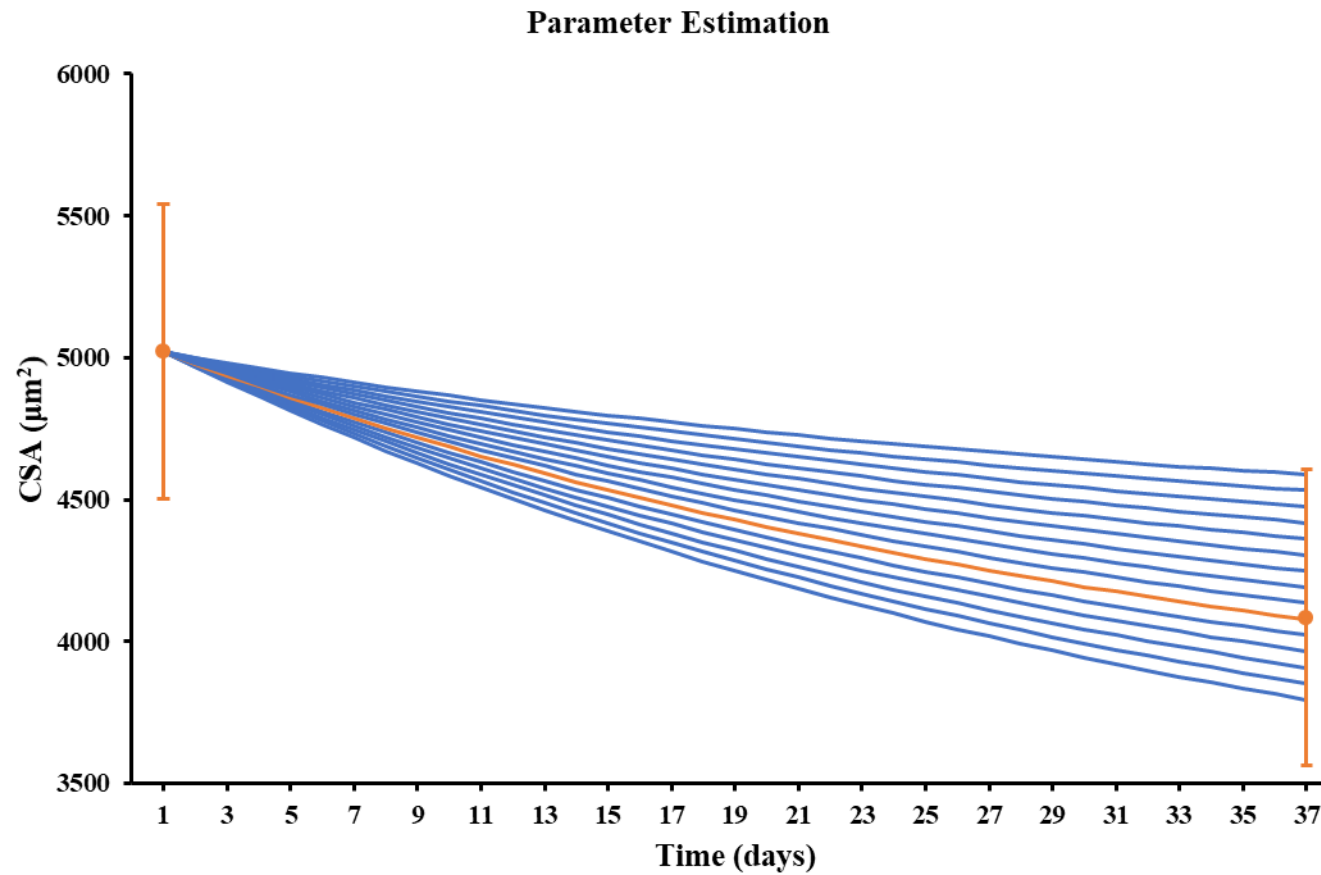


**Figure 3.3 Parameter Estimation**

Changes in fiber area during bed rest atrophy was simulated over a range of synthesis and degradation coefficients. Percent error was used to determine coefficients that best fit fiber area changes observed Berg et al., 1997.

*Determining protein metabolism during physical activity.*

Metabolic changes due to physical activity were modeled as transient increases in the protein synthesis and degradation coefficients. As previously discussed in Chapter 2, after a single bout of RE, protein synthesis is increased 100% while protein degradation is increased 40% (see Figure 3.4) (Phillips et al., 1997; Biolo et al., 1995). These changes were simulated by increasing  $\beta_s$  and  $\beta_d$  coefficients by 100% and 40% respectively and were assumed the same for all fiber types.

Fiber hypertrophy was modeled using the same differential equation (E1) as before, when protein synthesis exceeded protein degradation. The maximum hypertrophy rate (where all fibers are recruited and exercised until fatigued) was determined by varying the maximum  $\beta_s$  and  $\beta_d$  coefficient values until changes in fiber area closely matched those observed experimentally. All fiber types were assumed to be fully recruited at 90% MVC (Campos et al., 2002). Therefore, the rate at which each fiber type hypertrophied at 90% MVC was defined as the maximum hypertrophy rate for that fiber. Biopsy measurements of initial fiber areas were prescribed to model fibers as starting conditions (Campos et al., 2002). The maximum synthesis and degradation rates were then varied for each fiber type until there was a < 1% error between final simulated fiber areas and final experimental fiber areas.

By viewing daily activity as a low intensity form of resistance exercise, transient changes in protein metabolism associated with daily activity was modeled similarly to those from RE—just to a lesser degree. Protein metabolism during daily activity was determined by tuning increases in protein synthesis and degradation coefficients to match the experimental control group in a RE study until there was a percent error of <1% (Harber et al., 2004). These rates



were then validated using the control group from a second independent RE study (Campos et al., 2002).

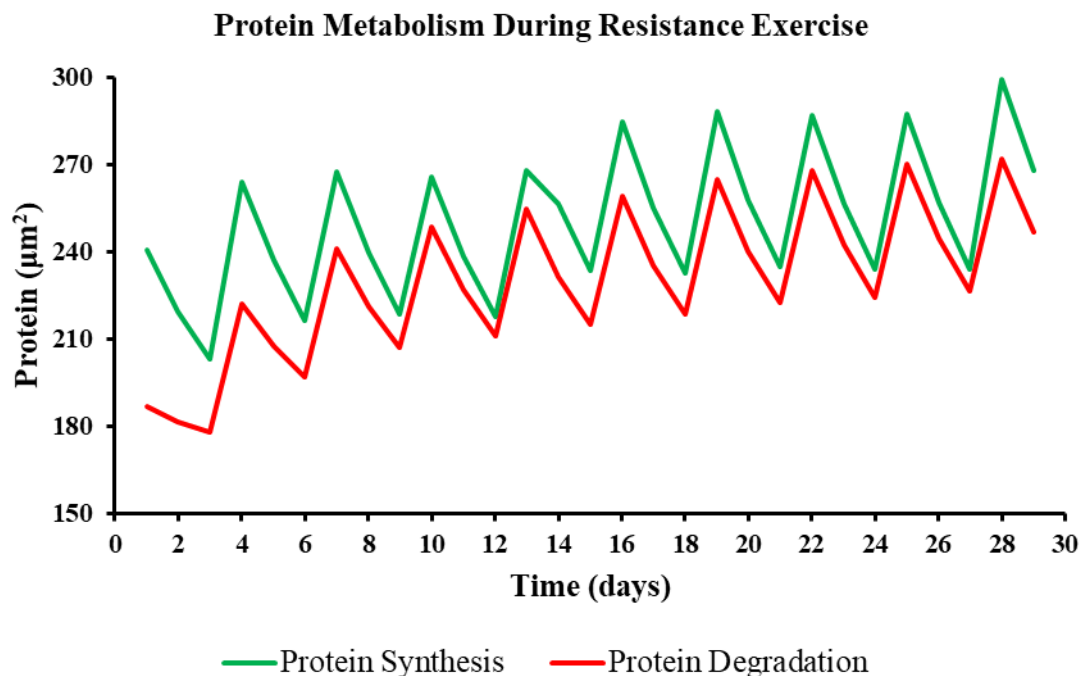


**Figure 3.4 Simulated Protein Metabolism During Physical Activity**

Transient increases in protein synthesis and degradation in response to resistance exercise. Both protein synthesis and degradation decline by 1/3 each day of rest.

*Determining fiber recruitment during RE.*

Since individual muscle fiber recruitment is not generally measured or reported in experimental studies, the relationship between fiber recruitment and RE intensity needed to be estimated. The recruitment of each fiber type was assumed to be a linear function of exercise intensity and was computed by using the fraction of weekly protein deposition ( $PD/PD_{max}$ ) as a proxy for the percentage of the fibers were recruited. First, the maximum weekly protein deposition rate ( $PD_{max}$ ) was computed by averaging the changes in fiber CSA over the course of a high intensity (~90% MVC) RE regime, where it was assumed all fibers were recruited

(Campos et al., 2002). RE intensity (% MVC) was estimated according to the relationship between the number of repetition maximums and % MVC (Reynolds et al., 2006).

$$PD_{\max} = \frac{CSA_{\text{final}} - CSA_{\text{initial}}}{\text{weeks}}$$

Similar calculations were used to determine the rates of protein deposition during RE hypertrophy in four additional RE regimes spanning a range of intensities from ~46% MVC to ~78% MVC (Campos et al., 2002; Harber et al., 2004; Green et al., 1998). These rates were plotted together and a linear regression was performed to determine the relationship between weekly protein deposition and intensity level (Figure 3.5). Finally, these linear functions were then normalized by the  $PD_{\max}$  to estimate fiber recruitment as a function of RE intensity.

As seen in Figure 3.6, Type I fiber recruitment was determined to be:  $R = 0.0096 * I + 0.1458$ , whereas Type IIA and IIB fiber recruitment was estimated as  $R = 0.0106 * I + 0.0543$  and  $R = 0.0125 * I - 0.109$  respectively, where “R” represented the percentage of fibers that were recruited and “I” represented RE intensity (% MVC) (Equations 9-11). All fibers types were assumed maximally recruited at 90% MVC. As expected according to the size principle, Type I fibers are recruited first, followed by Type IIA and then Type IIB fibers.

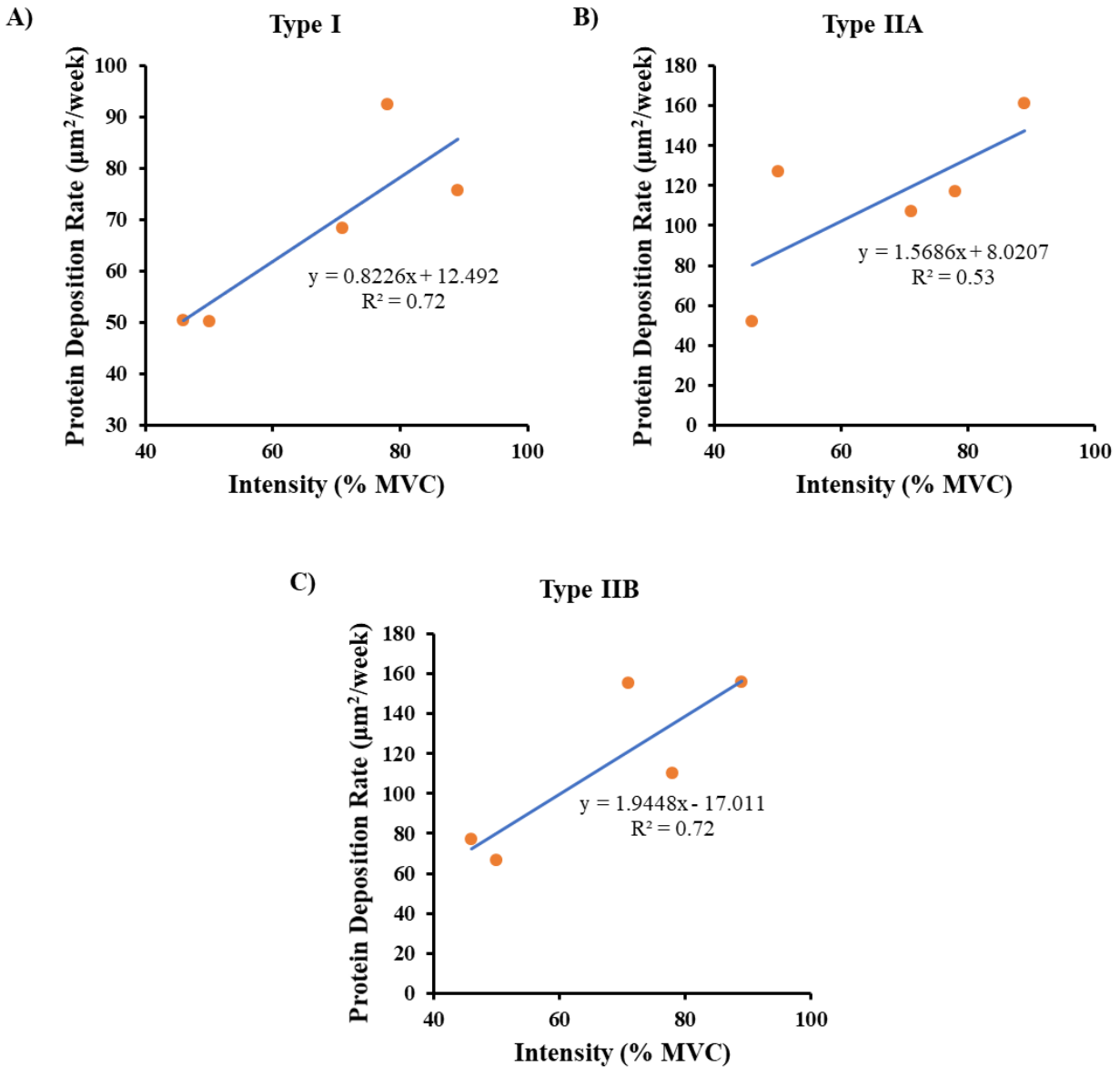


### Figure 3.5 Estimation of Fiber Recruitment

A linear regression of protein deposition rate ( $\mu\text{m}^2/\text{week}$ ) and RE intensity (% MVC) was performed to estimate fiber recruitment as a function of RE intensity for A) Type I, B) Type IIA, C) Type IIB fibers. The protein deposition rate was assumed to be a proxy for the number of recruited fibers maximally producing protein during RE (Campos et al., 2002; Harber et al., 2004; Green et al., 1998).

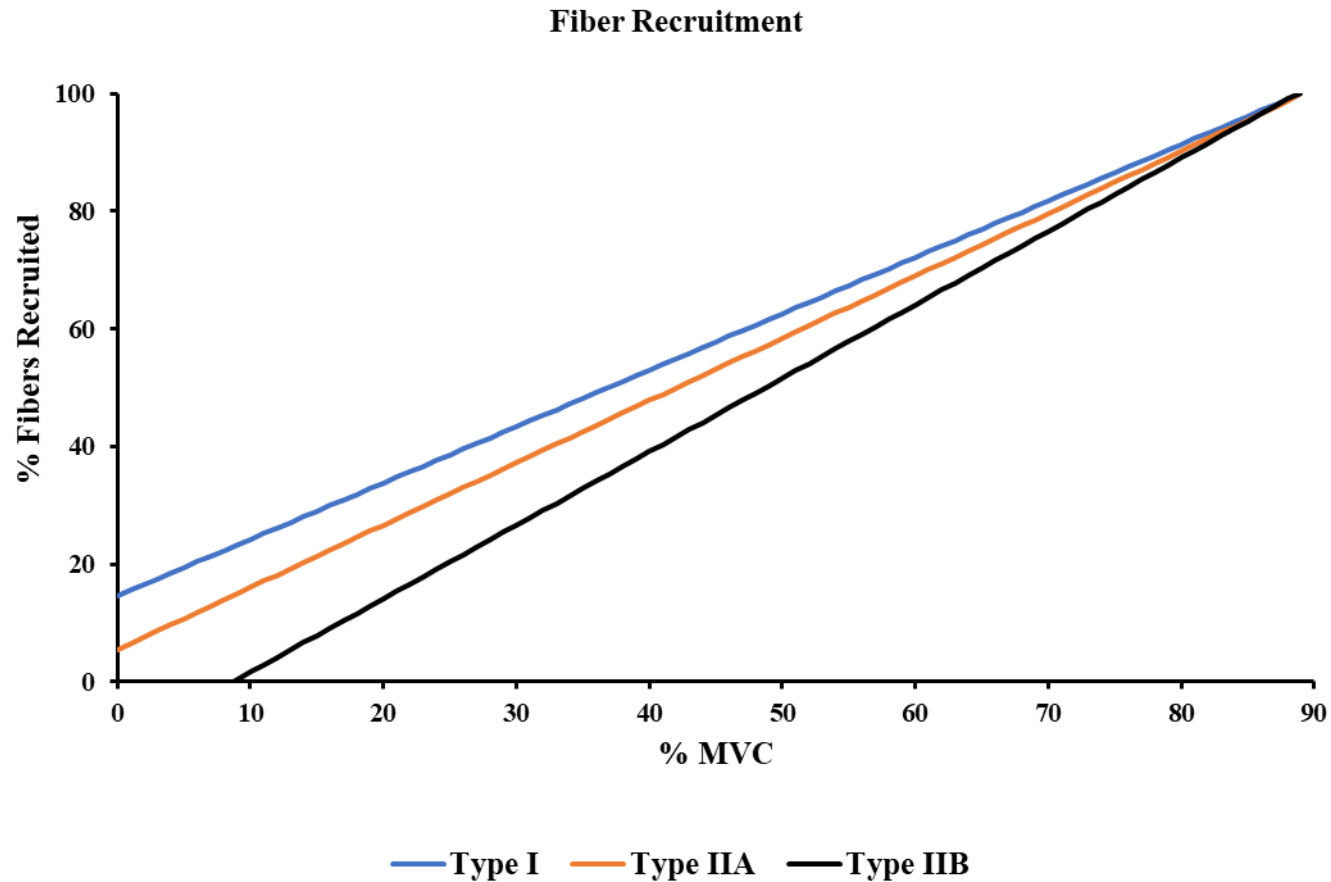


**Figure 3.6 Estimation of Fiber Recruitment**

Fiber Recruitment as a function of % MVC for each fiber type. Type I fibers (blue) are recruited first, followed by Type IIA fibers (orange), and Type IIB fibers (black). Recruitment patterns successfully mimic Hennemans' Size Principle where smaller motor units, primarily consisting of Type I fibers are recruited first, followed by larger motor units consisting of more Type IIA and IIB fibers.

### 3.4 Simulations of Muscle Adaptation Across A Range of Muscle Groups

Fiber type distributions and initial CSA for 29 muscle groups were used as initial conditions to simulate muscle adaptation during eight weeks of bed-rest atrophy and eight weeks of RE (Johnson et al., 1973; Polgar et al., 1973). The prescribed RE regime was set at 80% with two days of rest between each bout of exercise. Normalized change for each muscle group was calculated to determine how different muscle groups with various architecture responded to the same physical activities ( $Normalized\ change = 1 - CSA(t) / initial\ CSA$ ). Since the data from Johnson et al. and Polgar et al. only included measurements for Type I and II fibers, the percentages of Type IIA and IIB fibers were each assumed to be equal to half the percentage of Type II fibers. Additionally, the CSA of Type II fibers were assigned as initial conditions to both Type IIA and IIB fibers.

### 3.5 Simulations of Muscle Adaptation Following Detraining and Subsequent Retraining

All fiber types were simulated over a period of detraining and subsequent retraining to determine if myonuclei retained during physical disuse enabled muscle fibers to quickly adapt to increased physical activity. Simulations sought to replicate published observations of the effect of 30-32 weeks detraining and subsequent accelerated hypertrophy during 6 weeks RE retaining on fiber CSA in women (Staron et al., 1991). Mean and standard deviations of fiber CSAs from the experimental subjects after 20 weeks of initial RE training were used as initial conditions for the simulations. Model fibers were simulated for 31 weeks of bed-rest atrophy, followed by six weeks of RE retraining at 80% MVC with two days of rest between each bout of RE. An one-way ANOVA was run to analyze significant differences between the simulated CSAs for the three time points, followed by a Turkey HSD to determine which groups' means were different.

## 4 Results

This chapter outlines the results generated when building the ABM, including model parameters, as well as simulations of muscle adaptation. These model parameters include baseline protein metabolism rates, changes in protein metabolism to daily activity, maximum protein metabolism rates associated with RE, and fiber type recruitment as a function of RE intensity. A summary of resulting model parameters is presented in Table 4.1. These parameters were then used to simulate muscle adaptation (eight weeks of muscle atrophy and hypertrophy respectively) of 29 different muscles as well as how muscle adapts to detraining and subsequent retraining. An analysis of these simulations is presented.

**Table 4.1 Model Parameters**

Fiber Type	Model Parameter
<i>Baseline Rates</i>	Baseline protein metabolic rates from bed rest atrophy.
Type I	$\beta_s \text{ baseline} = 41$ $\beta_d \text{ baseline} = 0.0288$
Type IIA	$\beta_s \text{ baseline} = 48$ $\beta_d \text{ baseline} = 0.0288$
Type IIB	$\beta_s \text{ baseline} = 42$ $\beta_d \text{ baseline} = 0.0288$
<i>Daily Activity</i>	Transient increases in protein metabolism due to daily activity.
Type I	$\beta_s \text{ inc} = 0.18$ $\beta_d \text{ inc} = 0.06$
Type IIA	$\beta_s \text{ inc} = 0.1$ $\beta_d \text{ inc} = 0.06$
Type IIB	$\beta_s \text{ inc} = 0.13$ $\beta_d \text{ inc} = 0.05$
<i>Maximum Rates</i>	Maximum protein metabolism dictating the rate at which muscles can hypertrophy.
Type I	$\beta_s \text{ max} = 137$ $\beta_d \text{ max} = 0.085$
Type IIA	$\beta_s \text{ max} = 148$ $\beta_d \text{ max} = 0.085$
Type IIB	$\beta_s \text{ max} = 147$ $\beta_d \text{ max} = 0.085$

## 4.1 Model Parameters

### *Synthesis and degradation coefficients for bed rest atrophy*

When baseline synthesis and degradation coefficients were varied to simulate bed-rest atrophy, synthesis coefficients ( $\beta_s$ ) of 41, 48, 42  $\mu\text{m}^2/\text{nuclei}^{-1} \cdot \text{day}^{-1}$  for Types I, IIA, and IIB respectively and degradation coefficients ( $\beta_d$ ) of 0.0288  $\text{day}^{-1}$  for all fiber types matched observed final fiber CSAs within < 1% error (Berg et al., 1997). These rates were then validated against CSA decreases from independent bed rest atrophy studies (Figure 4.1) (Bamman et al., 1998; Widrick et al., 1997). Atrophy coefficients for Type IIA and IIB fibers were averaged and validated using Type II fiber CSA decreases as observed in Bamman et al.  $\beta_s$  and  $\beta_d$  coefficient values for all fiber types were within the standard deviations for these studies and were therefore deemed acceptable. These coefficients were then used as baseline values for all future simulations.

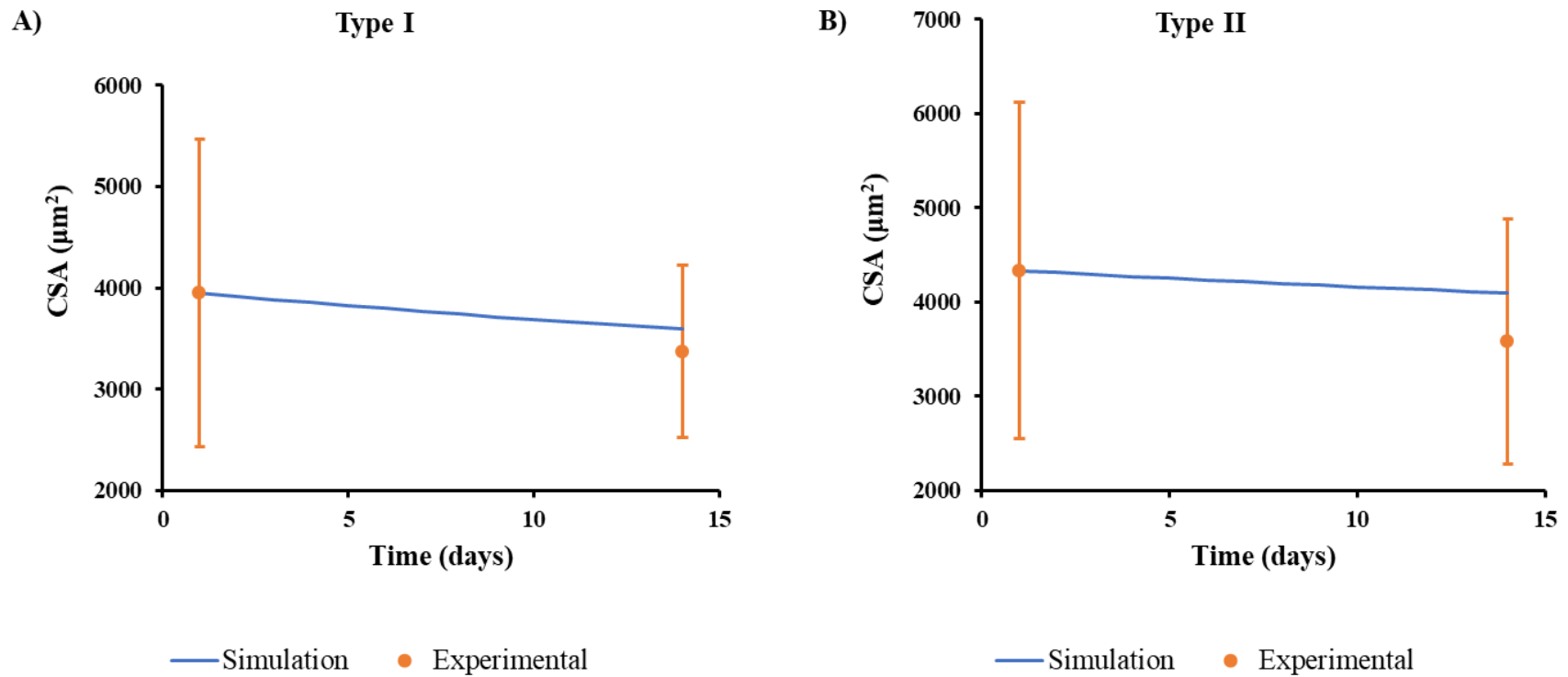


#### Figure 4.1 Atrophy Parameter Validation

Muscle atrophy was validated using independent experimental data from Bamman et al., 1998 and Widrick et al., 1997. Simulated muscle sizes were within standard deviations of the experimental values.



### *Protein metabolism during daily activity*

The model predicted that protein synthesis increases during daily activity were 18% for Type I, 10% for Type IIA, and 13% for Type IIB. Degradation increases were 6% for Type I, 6% for Type IIA, and 5% for Type IIB. These transient increases in protein metabolism due to daily physical activity were used in all future simulations where bed-rest was not prescribed.

### *Protein metabolism during resistance exercise-induced hypertrophy*

Maximum synthesis rates limiting muscle fiber hypertrophy RE were  $136 \mu\text{m}^2/\text{nuclei}^{-1} * \text{day}^{-1}$  for Type I fibers,  $148 \mu\text{m}^2/\text{nuclei}^{-1} * \text{day}^{-1}$  for Type IIA fibers, and  $147 \mu\text{m}^2/\text{nuclei}^{-1} * \text{day}^{-1}$  for Type IIB fibers. It should be noted that these values for maximum synthesis rates represent the myonuclei's protein synthesis capacities for each fiber type. Maximum degradation rates during RE hypertrophy were  $0.085 \text{ day}^{-1}$  for Type I fibers,  $0.085 \text{ day}^{-1}$  for Type IIA fibers, and  $0.085 \text{ day}^{-1}$  for Type IIB fibers. It was observed that fiber types IIA and IIB have higher myonuclei synthesis capacities than Type I fibers. By analyzing each fibers' maximum synthesis and degradation rates, the model predicts that Type IIA and IIB fibers have the potential to hypertrophy more quickly than Type I fibers, validating published RE observations that Type II fibers exhibit the greatest response to RE training (Fry, 2004). These values for maximum synthesis and degradation rates were then used to determine fiber recruitment as detailed in Chapter 3.

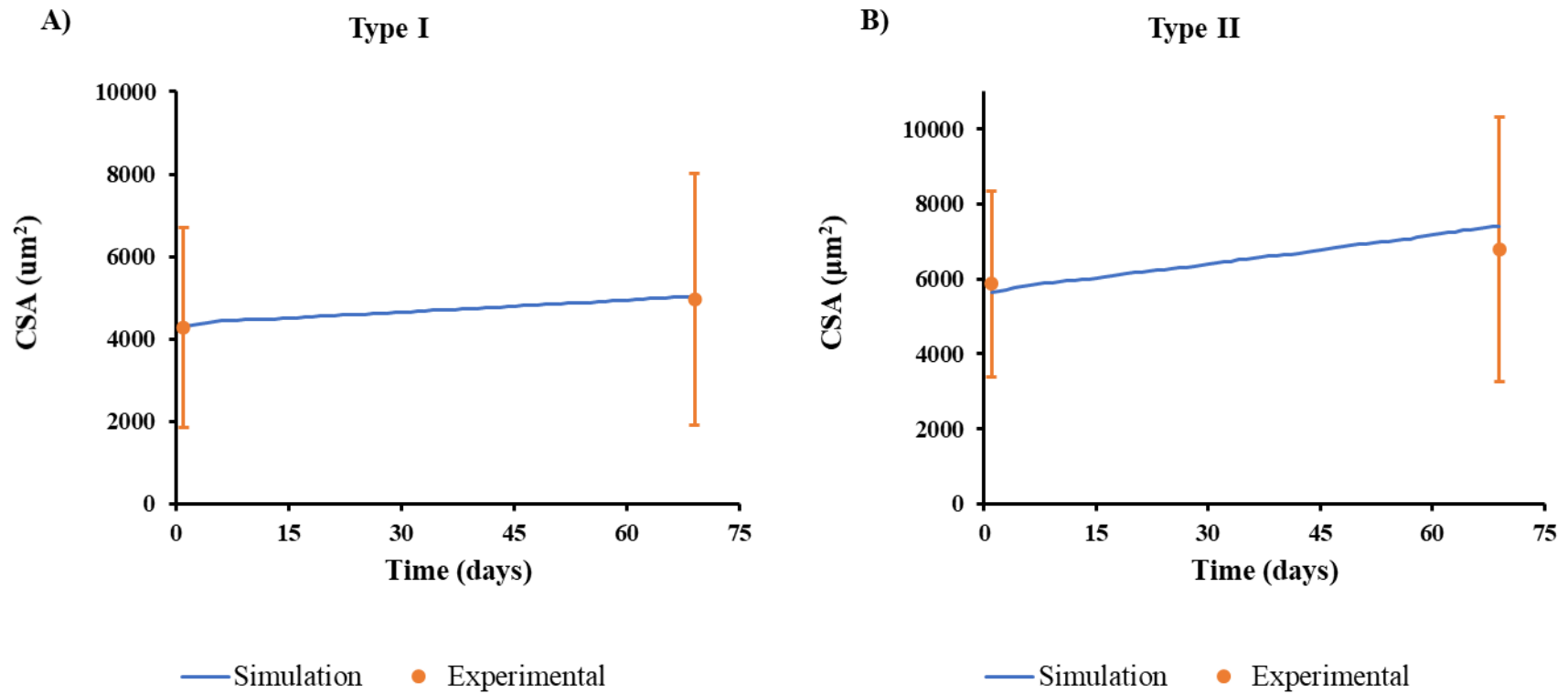


**Figure 4.2 Hypertrophy Parameter Validation**

Muscle hypertrophy was validated for each fiber type using independent experimental data from Mitchell et al., 2012. Simulated muscle sizes were within standard deviations of the experimental values.

## 4.2 Muscle Architecture Determines Muscle Adaptation

Using the validated model parameters, eight weeks of bed-rest atrophy and eight weeks of RE hypertrophy were simulated to determine how 29 different muscles with various architectures adapted to the same physical activities. Each muscles' initial fiber type distribution and CSA were prescribed based on experimental observations (Johnson et al., 1973; Polgar et al., 1973). The model simulated a range of normalized atrophy from 21.6 to 25.9% and normalized hypertrophy from 9.7 to 17.5% (see Figure 4.4). The extensor digitorum brevis muscle exhibited the least atrophy as well as the greatest hypertrophy, whereas the Pectoralis Major muscle atrophied to the greatest extent and hypertrophied the least. All 29 muscles were then clustered using Euclidean shortest-distance analysis by fiber type distribution and initial CSA to determine if muscle architecture influenced the degree of atrophy and/or hypertrophy. Muscles were clustered into 3 major groups. Analyzing these cluster groups, revealed that muscles with similar architectural properties atrophied and hypertrophied to similar degrees.

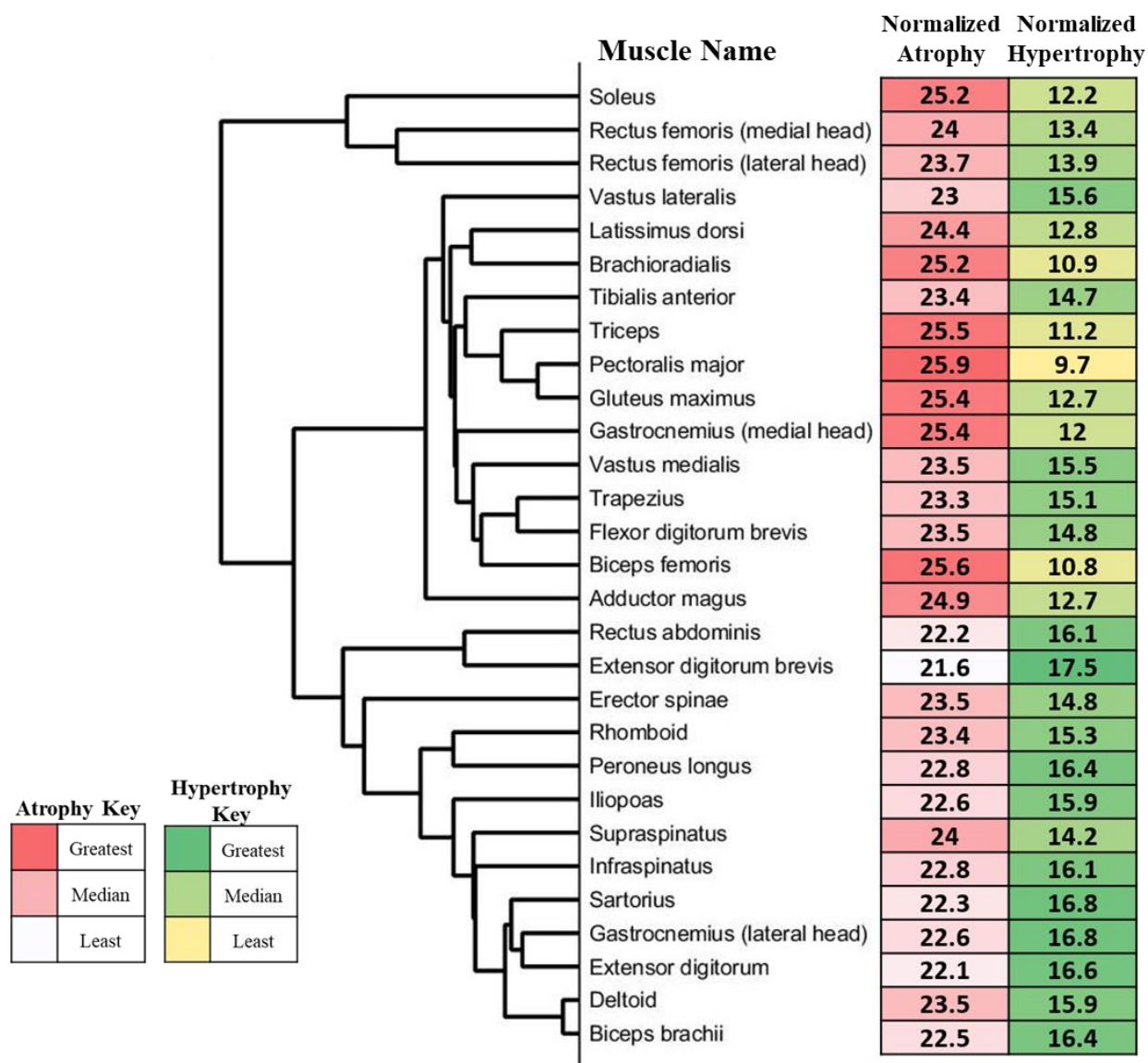


**Figure 4.3 Euclidean Shortest Distance Dendrogram**

On the left is a Euclidean shortest-distance hierarchical clustering of 29 muscles were based on initial fiber type distribution and CSA (data from Johnson et al., 1973; Polgar et al., 1973). On the right is simulated normalized atrophy and hypertrophy. Muscles clustered together exhibit similar degrees of muscle adaptation.

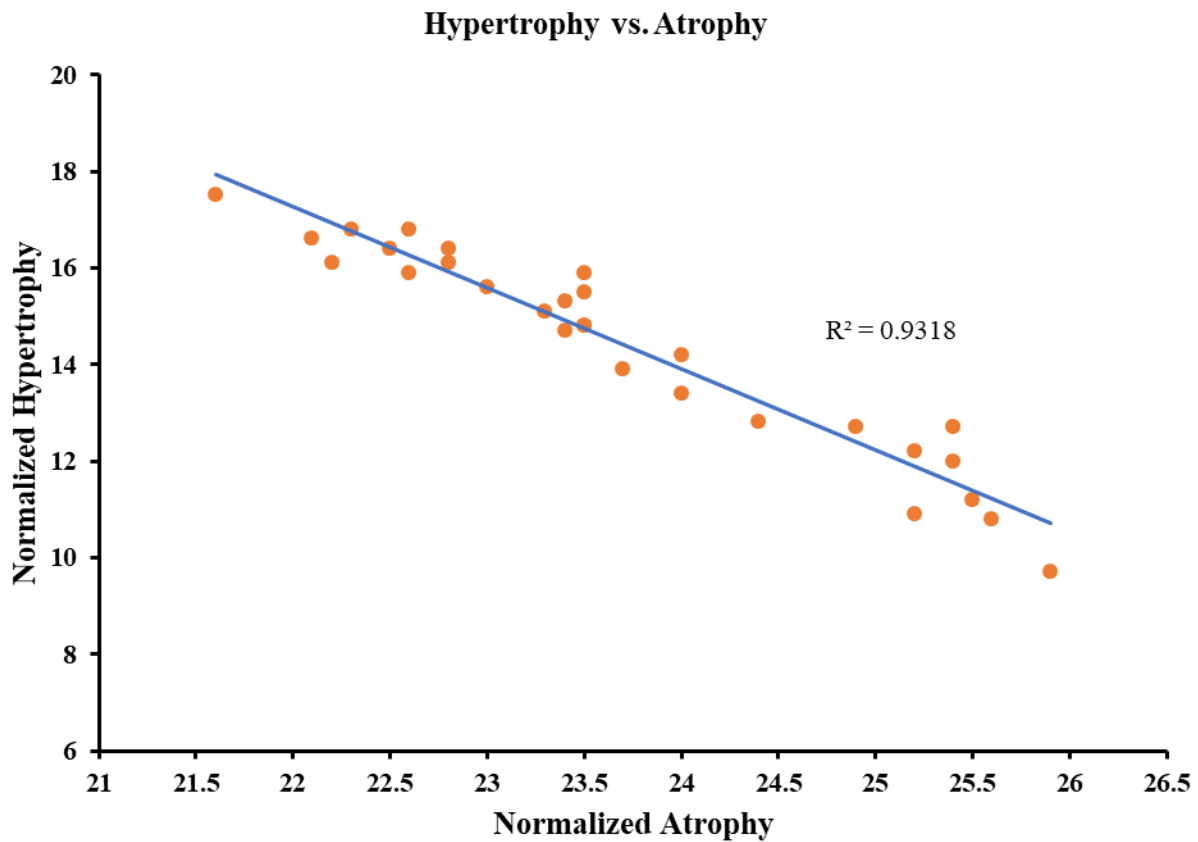


**Figure 4.4 Correlation Between Simulated Hypertrophy and Atrophy**

There is a significant correlation between simulated normalized hypertrophy and normalized atrophy for 29 muscle groups ( $R^2 = 0.9318$ ;  $p < 0.01$ ). This indicates that muscles that are more prone to muscle hypertrophy are more atrophy-resistant.

Interestingly, simulated normalized atrophy and hypertrophy were inversely related. As seen in Figure 4.5, normalized atrophy and hypertrophy were significantly correlated ( $R^2 = 0.9318$ ;  $p < 0.001$ ), suggesting that muscles that are more prone to atrophy or hypertrophy based on initial architecture. This could indicate specialization amongst muscles based on function.

In order to determine which architecture parameters most accurately predicted muscle adaptation, the six fiber parameters (fiber type percentages and initial CSA for each fiber type) were correlated with normalized hypertrophy and atrophy. These correlations generated six scatter plots for each hypertrophy and atrophy. Percentages of fiber types I, IIA, and IIB were significantly correlated ( $p < 0.05$ ) with normalized hypertrophy ( $R^2 = 0.66$  for each; see Figure 4.6). Initial CSA of Type I fibers was significantly correlated with normalized hypertrophy ( $R^2 = 0.26$ ). However, initial Type IIA and IIB CSAs were not significantly correlated. A multiple regression including fiber type percentage as well as initial CSA for all fiber types most accurately correlated to normalized hypertrophy ( $R^2 = 0.90$ ). Therefore, while the overall muscle architecture is the best predictor of muscle hypertrophy, the distribution of fiber types as well as the initial CSA of Type I fibers predicts the degree to which an individual muscle hypertrophies. For muscle atrophy, fiber type percentage for any fiber was not significantly correlated (see Figure 4.7). However, initial CSA of all fiber types were significantly correlated (Type I:  $R^2 = 0.28$ ,  $p = 0.003$ ; Type IIA:  $R^2 = 0.33$ ,  $p = 0.001$ ; Type IIB  $R^2 = 0.33$ ,  $p = 0.001$ ). A multiple regression consisting of all architecture parameters was not a more accurate predictor of muscle atrophy. Therefore, the initial fiber CSA for each fiber type is the best predictor of muscle atrophy.

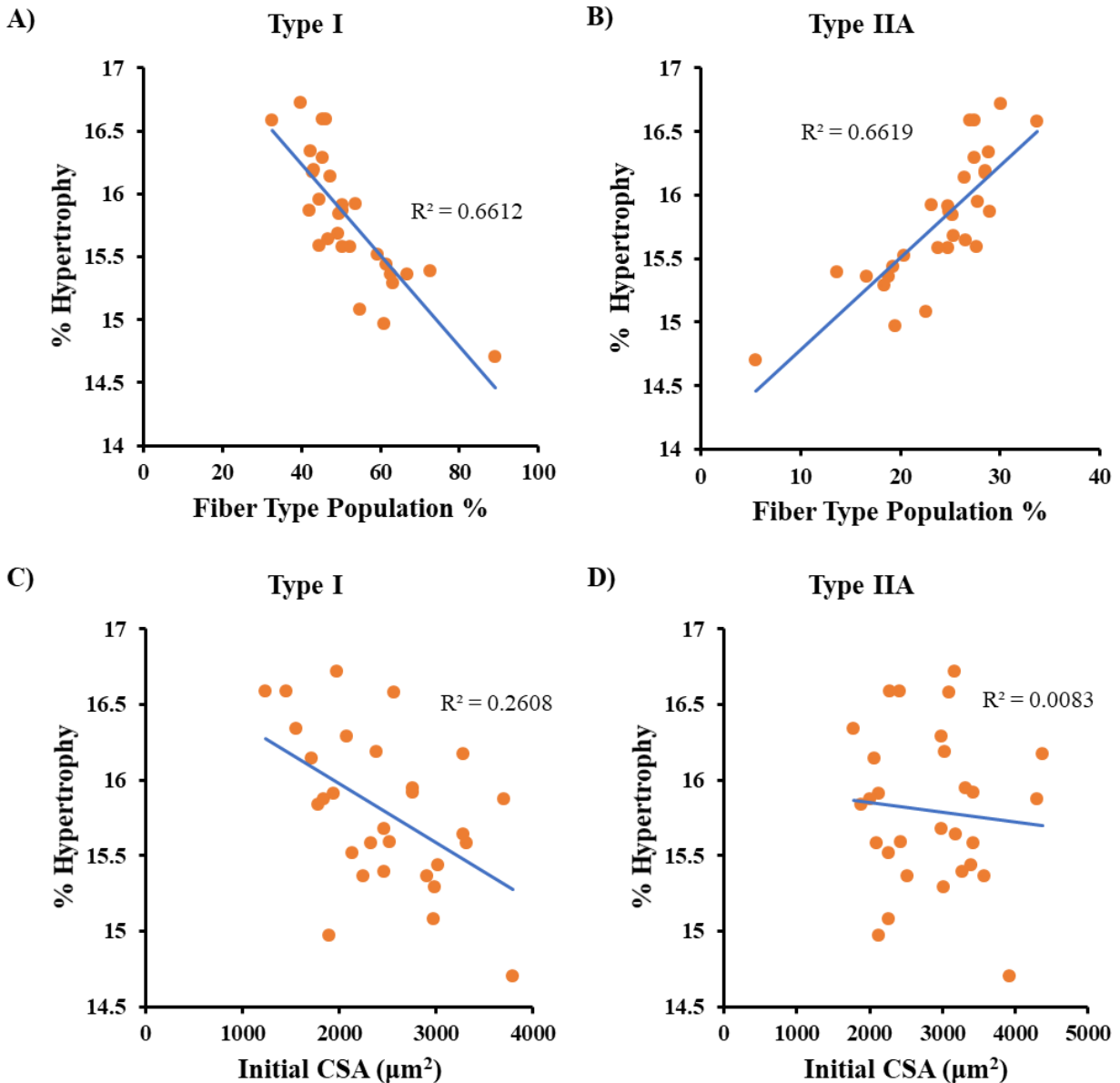


**Figure 4.5 Muscle Architecture Can Predict Hypertrophy**

Scatter plots of fiber type distribution vs. hypertrophy (A and B) and initial fiber CSA vs. hypertrophy (C and D) for Types I and IIA fibers (Type IIB not shown). Hypertrophy is significantly correlated with fiber type distributions (Type I:  $R^2 = 0.66$ , Type IIA:  $R^2 = 0.66$ , Type IIB:  $R^2 = 0.66$ ). Muscle hypertrophy is not significantly correlated with initial fiber CSA.

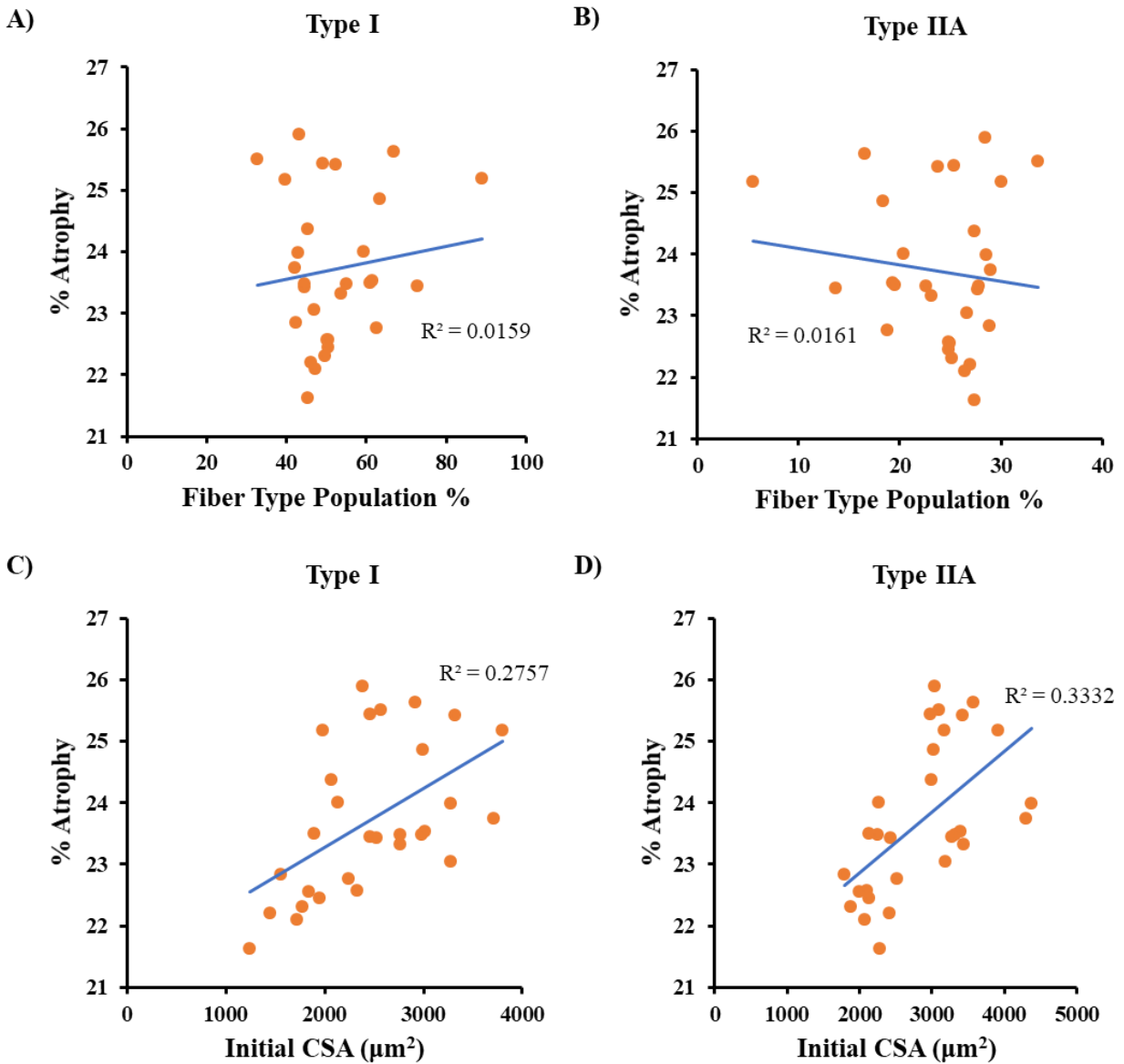


**Figure 4.6 Muscle Architecture Can Predict Atrophy**

Scatter plots of fiber type distribution vs. atrophy (A and B) and initial fiber CSA vs. atrophy (C and D) for Types I and IIA fibers (Type IIB not shown). Atrophy is significantly correlated with initial fiber CSA (Type I:  $R^2 = 0.28$ , Type IIA:  $R^2 = 0.33$ , Type IIB:  $R^2 = 0.33$ ). Muscle atrophy is not significantly correlated with initial fiber type distribution.



### **4.3 Model Simulations of Detraining and Retraining Support Theory of Muscle Memory**

Simulations of muscle fiber detraining and retraining validate experimental observations that muscle fibers are able to more quickly adapt to retraining after a period of detraining by maintaining their myonuclei during disuse (Staron et al., 1991). A Student's t-test was conducted to determine if simulated fibers were significantly different from experimental observations at each time point. At all time points, simulated fibers were not significantly different than experimental data ( $p > 0.05$ ). Additionally, simulations accurately predicted observed muscle adaptation. At 31 weeks of detraining, Type IIA and IIB fiber CSA was significantly decreased from the initial starting conditions ( $p < 0.01$ ). These values match experimental observations where Type IIB fibers were significantly decreased at this time point, and Type IIA fibers did exhibit noticeable decreases in CSA. After six weeks of simulated retraining, all simulated fibers were significantly greater than their respective detrained values ( $p < 0.01$ ). These simulations matched observed data for Types IIA and IIB fibers. The rapid hypertrophy response of fiber area to retraining after an extended period of detraining demonstrates the effectiveness of maintaining myonuclei during muscle disuse, as fibers are able to quickly adapt to increases in physical demand. If myonuclei were not maintained during the period of detraining, muscle fibers would take much longer than the observed 6 weeks of retraining to regain initial fiber. Therefore, our simulations support the theory that by retaining myonuclei through periods of disuse, muscle fibers are able to respond to increased physical activity much quicker than if the myonuclei were removed.

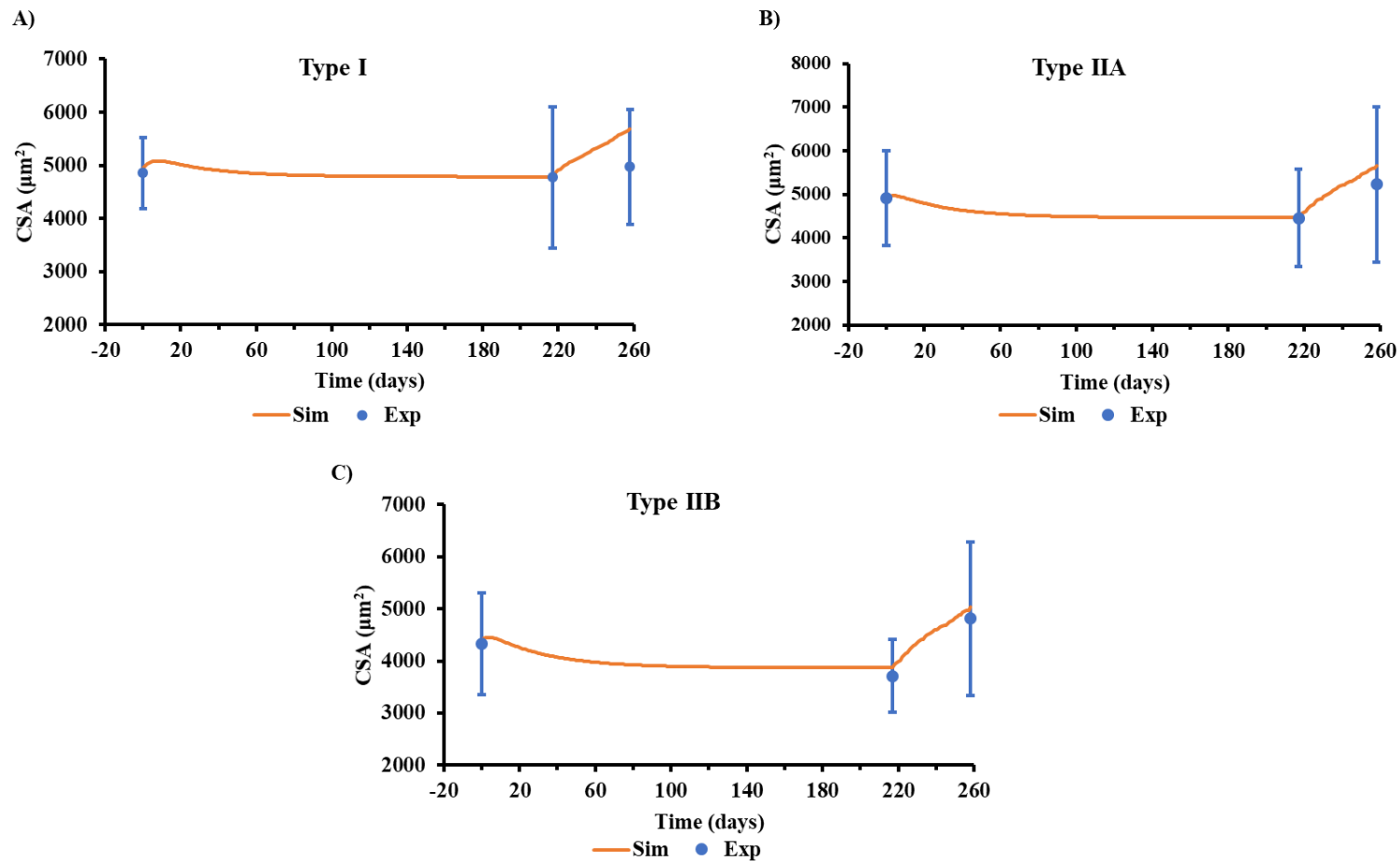


**Figure 4.7 Simulations of Detraining and Retraining**

Simulations of detraining and subsequent retraining support theory that myonuclei maintained during disuse enable muscle to quickly adapt to increases in physical activity. Initial mean and SD of fiber CSAs from Staron et al., 1991 were prescribed as initial conditions for simulations. Muscle fibers were detrained for 31 weeks, then retrained for six weeks. There were no significant differences between experimental and simulated results at each time point. Additionally, A) Simulated Type I fibers exhibited significant differences between detrain and retrain values ( $p < 0.01$ ). B) Simulated Type IIA fibers exhibited significant differences between initial and detrain values ( $p < 0.01$ ) as well as between detrain and retrain values ( $p < 0.01$ ). C) Simulated Type IIB fibers exhibited significant differences between initial and detrain values ( $p < 0.01$ ) as well as between detrain and retrain values ( $p < 0.01$ ).

## 5 Discussion

The goal of this study was to develop a computational model of the relationship between skeletal muscle adaptation and changes in physical activity. This goal was achieved by: 1) compiling experimental data on muscle adaptation, 2) postulating an activity-based differential equation that reflects macro insights on the cellular scale, 3) integrating that differential equation into a computational framework, and 4) validating empirically-derived parameters that could accurately predict muscle adaptation to various physical activities. This discussion provides an explanation of the results of model simulations and their implications, describes the significance of several assumptions and limitations of the methods used to develop the model, and proposes future directions for improving the understanding of the relationship between muscle adaptation to physical activity.

### 5.1 Summary and Implications

The ABM accurately simulated changes in fiber CSA consistent with experimental observations in response to bed rest-induced disuse atrophy, daily activity, and RE-induced fiber hypertrophy. Analysis of these simulations revealed that fiber adaptation to physical activity could be accurately represented by three parameters: protein synthesis per nuclei per day ( $\beta_s$ ), the rate of protein degradation per CSA ( $\beta_d$ ), and the number of myonuclei per fiber CSA. By altering these parameters in response to changes in physical activity, the proposed computational model can accurately simulate and predict observed muscle adaptation to physical activity.

Through parameter estimation, it was determined that each fiber type adapts to physical activity independently—fiber types I, IIA, and IIB do not atrophy and hypertrophy at the same rates in response to similar stimuli. During muscle atrophy, Type I and IIB fibers atrophy the

quickest. Type IIA fibers are most resistant to disuse atrophy as they produce a higher baseline net protein turnover rate. During muscle hypertrophy in response to RE, Type IIA and IIB fibers grow the quickest, followed Type I fibers. These observations of fiber adaptation demonstrate that Type IIB fibers are the most responsive fiber type to changes in physical activity—they atrophy the quickest in response to disuse and hypertrophy the quickest in response to resistance exercise. Additionally, Type I fibers are most responsive to daily activity [Equation 2]. This result is consistent with theoretical fiber recruitment strategies, where in low intensity activity, Type I fibers would be recruited first (Garnet et al., 1979). Additionally, since Type IIA and IIB fibers do exhibit transient increases in protein metabolism as a result of daily activity, they are recruited. This result compliments fiber recruitment strategies estimated in the model where Type IIA fibers are recruited at any intensity while Type IIB fibers are recruited once intensity levels are above 10% MVC [Equations 9-11]. These recruitment equations are, to our knowledge, the first computational estimations of fiber type recruitments as a function of physical activity intensity. Therefore, their functionality in predicting how fiber types respond to physical activity should be implemented in future analysis of fiber adaptation to increased physical activity.

With respect to the new muscle memory theory, it is important to consider the lifetime of myonuclei observed to have been retained during atrophy (Bruusgaard et al., 2012; Ohira et al., 1999; Kadi et al., 2004). Studies on human cellular turnover using Carbon isotopes have estimated that nuclei in the intercostal muscle tissue had an average age of 15.1 years (Spalding et al., 2005). However, as noted by Gunderson et al., 2016, this is a low-estimate of the lifespan of human myonuclei because this estimate included other cell type within muscle tissue that have much higher turnover rates. Additionally, these estimates were made in subjects of ages 37 and

38, where myonuclei could have also been added to their fibers from exercise relatively recently. Therefore, it is quite possible that myonuclei in skeletal muscle remain in muscle fibers much longer than the estimated 15.1 years. Cardiomyocytes for example, exhibit less than 50% turnover during a normal human lifespan (Bergmann et al., 2009). Therefore, in order to determine the how long the benefits of retaining myonuclei during disuse last, it is imperative for future studies to determine the turnover rate of myonuclei remain in skeletal muscle fibers. However, for the purpose of this study looking at timescales of much less than 15 years, the assumption that myonuclei are permanently retained during periods of disuse is justified. Therefore, according to our proposed differential equation (Equation 1), any resistance exercise resulting in myonuclear addition has long-lasting implications for fiber CSA size. As seen in Equation 2, fiber CSA limitations over time is proportional to the number of myonuclei per fiber. Therefore, any increases in myonuclei count increases the minimum CSA of muscle fibers. This could have profound implications of the importance of RE as a measure to prevent muscle atrophy associated with age (sarcopenia). If myonuclei are added to muscle fibers while myonuclear addition is still efficient, sarcopenia in older age can be attenuated. While this theory is still developing, it represents a promising strategy to proactively treat sarcopenia. Therefore, more research on this topic should be conducted to ascertain if this is a valid preventative measure.

## **5.2 Assumptions and Limitations**

When assessing the relevance of any computational model, it is important to consider assumptions and limitations imbedded when constructing the model. The first consideration that needs to be made when examining the results of this study is that the model was constructed using only studies analyzing men 25-35 years of age. This assumption was important to make

while constructing the model in order to reduce variability seen between fiber adaptations between men and women as well as between the young and the elderly. Especially in cases of muscle hypertrophy to RE, men have been observed to hypertrophy quicker than women (Petrella et al., 2006). It is possible that men have a higher synthesis capacity per myonuclei than women. Future studies and analysis on this topic need to be pursued before translating these results to fiber adaptation in women. Additionally, it has been observed that hypertrophy is diminished in elderly populations due to decreased efficiency in myonuclei distribution throughout the fiber as well as a reduced ability to activate quiescent satellite cells (Van der Meer et al., 2011; Petrella et al., 2006). This in turn inhibits protein synthesis, making it more difficult to hypertrophy and elicit myonuclear addition. The current model framework does not account for how myonuclei are distributed in muscle fibers and assumes that myonuclei are distributed evenly throughout the fiber. However, the flexibility of agent-based modeling allows future adaptations such as tracking myonuclei and their contributions throughout muscle fibers. Therefore, I advocate that by expanding upon this framework can allow further insight into how the distribution of myonuclei throughout a muscle fiber can affect upkeep and hypertrophy.

In addition to the current framework only simulating fiber adaptations for young men, nutrition was not considered during fiber growth and upkeep. Receiving various amounts of protein during diet has been seen to inhibit fiber growth and upkeep. This model currently assumes that the subject is receiving enough protein in their diet to elicit changes observed experimentally. In order to analyze the effect of nutrition of fiber adaptation, nutritional data needs to be incorporated into the model. For the scope of this model, analyzing healthy muscle adaptation to changes in physical activity, adding nutritional requirements was unnecessary.

However, as previously mentioned, this framework is flexible enough to allow the addition of nutritional requirements to determine how this could affect proper muscle hypertrophy.

Finally, another limitation of the model that needs to be considered is the model does not simulate the addition of new fibers and does not convert the fiber's type during changes in activity. Studies have shown that fibers can be added to muscle fascicles through fusion of satellite stem cells—known as hyperplasia. The effects of hyperplasia on fascicle CSA changes were not addressed, but may significantly alter simulated muscle growth on the tissue level. Additionally, fiber type conversions have been observed during different physical activities (Fry, 2004). It has been theorized that Type IIB fibers convert to Type IIA during exercise to increase the fatigue-resistance of muscle fibers (Fry, 2004). Such changes could increase the efficiency of muscle functionality as muscle will become more specified to perform required tasks. Adding these rules to the existing framework could provide further insight into how muscle tissue as a whole adapts to physical activity.

### **5.3 Contributions and Future Work**

This computational framework provides a novel tool for describing the relationship between skeletal muscle adaptation and changes in physical activity in humans. It was built by postulated an activity-based differential equation that reflects macro insights on the cellular scale and validated the framework using empirically-derived parameters that accurately predict muscle adaptation to various physical activities. This model contributes a novel method for predicting changes in skeletal muscle for clinical populations such as bed-rest patients and subjects recovering from severe injuries.

In addition to providing a tool to improve our ability to predict muscle adaptation, this framework serves as a platform for future studies to build off of and as an effective instrument suggesting new experiments to improve understanding of muscle adaptation. The framework was designed as a simple differential equation imbedded in an agent-based model in order to be flexible enough to allow for future studies to use the model as base for exploration into more specific applications. Future additions that I recommend implementing include expanding the model to include muscle adaptation in women as well as in older populations as these are both important populations that often go understudied. In addition to adding adaptation methods for these populations, future iterations of the framework could look at how the addition of new fibers (hyperplasia) as well as fiber type conversions affect muscle adaptation.

Future attention should also be placed on improving understanding of the lifetime of myonuclei in skeletal muscle fibers. As previously mentioned, resistance training while younger with the purpose of efficiently adding myonuclei to muscle fibers could have profound importance as a preventative measure of preventing/attenuating sarcopenia. Therefore, more studies should seek to ascertain how long myonuclei are retained in adult muscle fibers. This information could prove crucial in mitigating the effects of aging by allowing the scientific community to better predict when is the optimal period for RE with the primary goal of acquiring myonuclei. In line with better understanding the lifetime of myonuclei during periods of disuse, future experiments should look at the effect retaining myonuclei on retraining. It may be possible for populations with extended periods of disuse atrophy to rapidly regain muscle size through retraining. Therefore, more studies should estimate the length of time muscles can atrophy due to disuse and still quickly hypertrophy due to retaining.



Another important direction for future studies is to evaluate and validate the quantitative estimates of fiber recruitment developed in this study. By better understanding how specific fiber populations are recruited during physical activity, future studies can seek to selectively target particular muscle groups to improve RE results or improve recovery from injury. Additionally, future studies should seek to determine if protein density is constant across all fiber type populations. For the scope of this study, protein density was assumed equal across all fiber types. However, since growth rates were trained and validated individually for each fiber type, this assumption was justified for this framework. However, if new experiments are able to delve deeper into protein density distribution across different fiber types, additions to this framework could be made to analyze more specifically the mechanisms of protein synthesis from myonuclei in each fiber type as well as how the MND in each fiber type could be affected.

## 6 References

- Adams, G.R., Caiozzo, V.J., Baldwin, K.M. Skeletal Muscle Unweighting: Spaceflight and Ground-Based Models. *Journal of Applied Physiology*. **95**(6), 2185-2201 (2003).
- Allen, D.L., Roy, R.R., Edgerton, V.R. Myonuclear Domains in Muscle Adaptation and Disease. *Muscle and Nerve*. **22**(10), 1350-1360 (1999).
- Bamman M.M., Clarke, M.S.F., Feedback, D.L., Talmadge, R.J., Stevens, B.R., Lieberman, S.A., Greenisen, M.C. Impact of Resistance Exercise During Bed Rest on Skeletal Muscle Sarcopenia and Myosin Inform Distribution. *Journal of Applied Physiology*. **84**(1), 157-163 (1998).
- Bawa, P., Binder, M.D., Ruenzel, P., Henneman, E. Recruitment Order of Motoneurons in Stretch Reflexes is Highly Correlated with Their Axonal Conduction Velocity. *Journal of Neurophysiology*. **52**(3), 410-420 (1984).
- Berg, H.E., Larsson, L., Tesch, P.A. Lower Limb Skeletal Muscle Function After 6 Wk of Bed Rest. *Journal of Applied Physiology*. **82**(1), 182-188 (1997).
- Bergmann, O., Bhardwai, R.D., Zdunek, S., Barnabe-Heider, F., Walsh, S., Zupicich, J., Alkass, K., Buchholz, B.A., Druid, H., Jovinge, S., Frisén. Evidence for Cardiomyocyte Renewal in Humans. *Science*. **324**(5923), 98-102 (2009).
- Biolo, G., Ciocchi, B., Lebenstedt, M., Barazzoni, R., Zanetti, M., Platen, P., Heer, M., Guarnieri, G. Short-Term Bed Rest Impairs Amino Acid-Induced Protein Anabolism in Humans. *Journal of Physiology*, **558**(2), 381-388 (2004).
- Biolo, G., Maggi, S.P., Williams, B.D., Tipton, K.D., Wolfe, R.R. Increased Rates of Muscle Protein Turnover and Amino Acid Transport After Resistance Exercise in Humans. *American Journal of Physiology*. **268**(3), E514-E520 (1995).
- Bodine, S.C., Stitt, T.N., Gonzalez, M., Kline, W.O., Stover, G.L., Bauerlein, R., Zlotchenko, E., Scrimgeour, A., Lawrence, J.C., Glass, D.J., Yancopoulos, G.D. Akt/mTOR Pathway is a Crucial Regulator of Skeletal Muscle Hypertrophy and Can Prevent Muscle Atrophy in Vivo. *Nature Cell Biology*. **3**, 1014-1019 (2001).
- Bruusgaard, J.C., Egner, I.M., Larsen, T.K., Dupre-Aucouturier, S., Desplanches, D., Gundersen, K. No Change in Myonuclear Number During Muscle Unloading and Reloading. *Journal of Applied Physiology*. **113**(2), 290-296 (2012).
- Burd, N.A., West, D.W.D., Staples, A.W., Atherton, P.J., Baker, J.M., Moore, D.R., Holwerda, A.M., Parise, G., Rennie, M.J., Baker, S.K., Phillips, S.M. Low-Load High Volume Resistance Exercise Stimulates Muscle Protein Synthesis More Than High-Load Low Volume Resistance Exercise in Young Men. *PLoS ONE*. **5**(8), (2010).
- Campos, G.E.R., Luecke, T.J., Wendeln, H.K., Toma, K., Hagerman, F.C., Murray, T.F., Ragg, K.E., Ratamess, N.A., Kraemer, W.J., Staron, R.S. Muscular Adaptations in Response to

- Three Different Resistance-Training Regimens: Specificity of Repetition Maximum Training Zones. *European Journal of Applied Physiology*. **88(1-2)**, 50-60 (2002).
- Chargé, S.B.P., Rudnicki, M.A. Cellular and Molecular Regulation of Muscle Regeneration. *Physiological Reviews*. **84(1)**, 209-238 (2004).
- Cheek, D.B. The control of cell mass and replication. The DNA unit - a personal 20-year study. *Early Human Development*. **12(3)**, 211-239 (1985).
- Cheek, D.B., Holt, A.B., Hill, D.E., Talbert, J.L. Skeletal Muscle Cell Mass and Growth: The Concept of the Deoxyribonucleic Acid Unit. *Pediatric Research*. **5**, 312-328 (1971).
- Damas, F., Phillips, S., Vechin, F.C., Ugrinowitsch, C. A Review of Resistance Training-Induced Changes in Skeletal Muscle Protein Synthesis and Their Contribution to Hypertrophy. *Sports Medicine*. **45(6)**, 801-807 (2015).
- Edgerton, V.R., Roy, R.R. Regulation of Skeletal Muscle Fiber Size, Shape, and Function. *Journal of Biomechanics*. **24(1)**, 123-133 (1991).
- Ferrando, A.A., Lane, H.W., Stuart, C.A., Davis-Street, J., Wolfe, R.R. Prolonged Bed Rest Decreases Skeletal Muscle and Whole Body Protein Synthesis. *American Journal of Physiology*. **270(4)**, E627-E633 (1966).
- Fry, A.C. The Role of Resistance Exercise Intensity on Muscle Fibre Adaptations. *Sports Medicine*. **34(10)**, 663-679 (2004).
- Garnett, R.A.F., O'Donovan, M.J., Stephens, J.A., Taylor, A. Motor Unit Organization of Human Medial Gastrocnemius. *Journal of Physiology*. **287(1)**, 33-43 (1979).
- Green, H., Goreham, C., Ouyang, J., Ball-Burnett, M., Ranney, D. Regulation of Fiber Size, Oxidative Potential, and Capillarization in Human Muscle by Resistance Exercise. *American Journal of Physiology Integrative Comparative Physiology*. **276(2)**, R591-R596 (1998).
- Gunderson, K. Muscle Memory and a New Cellular Model for Muscle Atrophy and Hypertrophy. *Journal of Experimental Biology*. **219(2)**, 235-242 (2016).
- Harber, M.P., Fry, A.C., Rubin, M.R., Smith, J.C., Weiss, L.W. Skeletal Muscle and Hormonal Adaptations to Circuit Weight Training in Untrained Men. *Scandinavian Journal of Medicine and Science in Sports*. **14(3)**, 176-185 (2004).
- Henneman E. Relation between size of neurons and their susceptibility to discharge. *Science*. **126(3287)**, 1345-1347. (1957)
- Henneman, E., Somjen, G., Carpenter, D.O. Excitability and inhibitability of motoneurons of different sizes. *Journal of Neurophysiology*. **28(3)**, 599-620 (1965a).
- Henneman E, Somjen, G., Carpenter, D.O. Functional significance of cell size in spinal motoneurons. *Journal of Neurophysiology*. **28(3)**, 560-580 (1965b).

- Hudson-Tole, E.F. and Wakeling, J.M. Motor Unit Recruitment for Dynamic Tasks: Current Understanding and Future Directions. *Journal of Comparative Physiology B*. **179(1)**, 57-66 (2009).
- Jackman, R.W. and Kandarian, S.C. The Molecular Basis of Skeletal Muscle Atrophy. *American Journal of Cell Physiology*. **287(4)**, C834-C843 (2004).
- Johnson, M.A., Polgar, J., Weightman, D., Appleton, D. Data on the Distribution of Fibre Types in Thirty-Six Human Muscles An Autopsy Study. *Journal of Neurological Sciences*. **18(1)**, 111-129 (1973).
- Kadi, F., Schjerling, P., Andersen, L.L., Charifi, N., Madsen, J.L., Christensen, L.R., Andersen, J.L. The Effects of Heavy Resistance Training and Detraining on Satellite Cells in Human Skeletal Muscles. *Journal of Physiology*. **588(3)**, 1005-1012 (2004).
- Karlsen, A., Couppé, C., Andersen, J.L., Mikkelsen, U.R, Nielsen, R.H., Magnusson, S.P., Kjaer, M., Mackey, A.L. Matters of Fiber Size and Myonuclear Domain: Does Size Matter More Than Age? *Muscle Nerve*. **52(6)**, 1040-1046 (2015).
- LeBlanc A.D., Schneider, V.S., Evans, H.J., Pientok, C., Rowe, R., Spector, E. Regional Changes in Muscle Mass Following 17 Weeks of Bed Rest. *Journal of Applied Physiology*. **73(5)**, 2172-2178 (1992).
- MacDougall, J.D., Sale, D.G., Always, E.E., Sutton, J.R. Muscle Fiber Number in Biceps Brachii in Bodybuilders and Control Subjects. *Journal of Applied Physiology*. **57(5)**, 1399-1403 (1984).
- Martin, K.S., Virgilio, K.M., Peirce, S.M., Blemker, S.S. Computational Modeling of Muscle Regeneration and Adaptation to Advance Muscle Tissue Regeneration Strategies. *Cells Tissues Organs*. **202(3-4)**, 250-266 (2015-2016).
- Martin, K.S., Blemker, S.S, Peirce, S.M. Agent-Based Computational Model Investigates Muscle-Specific Responses to Disuse-Induced Atrophy. *Journal of Applied Physiology*. **118(10)**, 1299-1309 (2015).
- McPhedran, A.M., Wurker, R.B., Henneman, E. Properties of Motor Units in a Heterogeneous Pale Muscle (M. Gastrocnemius) of the Cat. *Journal of Neurophysiology*, **28(1)**, 85-99 (1965a).
- McPhedran, A.M., Wurker, R.B., Henneman, E. Properties of Motor Units in a Homogeneous Red Muscle (Soleus) of the Cat. *Journal of Neurophysiology*, **28(1)**, 71-84 (1965b).
- Ohira, Y., Yoshinaga, T., Ohara, M., Nonaka, I., Yoshioka, T., Yamashita-Goto, K., Shenkman, B.S., Kozlovskaya, I.B., Roy, R.R., Edgerton, V.R. Myonuclear Domain and Myosin Phenotype in Human Soleus After Bed Rest with or Without Loading. *Journal of Applied Physiology*. **87(5)**, 1776-1785 (1999).
- Paddon-Jones, D., Sheffield-Moore, M., Cree, M.G., Hewlings, S.J., Aarsland, A., Wolfe, R.R., Ferrando, A.A. Atrophy and Impaired Muscle Protein Synthesis During Prolonged

- Inactivity and Stress. *The Journal of Clinical Endocrinology and Metabolism*. **91(12)**, 4836-4841 (2006).
- Pederson B.K., Febbraio, M.A. Muscles, exercise and obesity: skeletal muscle as a secretory organ. *Nature Reviews Endocrinology*. **8**, 457-465 (2012).
- Petrella, J.K., Kim, J., Cross, J.M., Kosek, D.J., Bamman, M.M. Efficacy of Myonuclear Addition May Explain Differential Myofiber Growth Among Resistance-Trained Young and Older Men and Women. *American Journal of Physiology Endocrinology and Metabolism*. **291(5)**, E937-E946 (2006).
- Petrella, J.K., Kim, J., Mayhew, D.L., Cross, J.M., Bamman, M.M. Potent Myofiber Hypertrophy During Resistance Training in Humans is Associated with Satellite Cell-Mediated Myonuclear Addition: A Cluster Analysis. *Journal of Applied Physiology*. **104(6)**, 1736-1742 (2008).
- Phillips, S.M., Tipton, K.D., Aarsland, A., Wolf, S.E., Wolfe, R.R. Mixed Muscle Protein Synthesis and Breakdown After Resistance Exercise in Humans. *American Journal of Physiology*. **273(1)**, E99-E107 (1997).
- Phillips, S.M., Glover, E.I., Rennie, M.J. Alterations of Protein Turnover Underlying Disuse Atrophy in Human Skeletal Muscle. *Journal of Applied Physiology*. **107(3)**, 645-654 (2009).
- Polgar, J., Johnson, M.A., Weightman, D., Appleton, D., Data of Fibre Size in Thirty-Six Human Muscles An Autopsy Study. *Journal of Neurological Sciences*. **19(3)**, 307-318 (1973).
- Reynolds, J.M., Gordon, T.J., Robergs, R.A. Prediction of One Repetition Maximum Strength from Multiple Repetition Maximum Testing and Anthropometry. *Journal of Strength and Conditioning Research*. **20(3)**, 584-592 (2006).
- Riek, S. and Bawa, P. Recruitment of Motor Units in Human Forearm Extensors. *Journal of Neurophysiology*. **68(1)**, 100-108 (1992).
- Sandri, M. Signaling in Muscle Atrophy and Hypertrophy. *Physiology*. **23(3)**, 160-170 (2008).
- Schiaffino, S., Dyar, K.A., Ciciliot, S., Blaauw, B., Sandri, M. Mechanisms Regulating Skeletal Muscle Growth and Atrophy. *FEBS Journal*. **280(17)**, 4294-4314 (2013).
- Scott, W., Stevens, J., Binder-Macleod, S.A. Human Skeletal Muscle Fiber Type Classifications. *Physical Therapy*. **81(11)**, 1810-1816 (2001).
- Snijders, T., Smeets, J.S.J., van Kranenburg, J., Kies, A.K., van Loon, L.J.C., Verdijk, L.B. Changes in Myonuclear Domain Size Do Not Precede Muscle Hypertrophy During Prolonged Resistance-Type Exercise Training. *Acta Physiology*. **216(2)**, 231-239 (2016).
- Spalding, K.L., Bhardwaj, R.D., Buchholz, B.A., Druid, H., Frisén, J. Restrospective Birth Dating of Cells in Humans. *Cell*. **122(1)**, 133-143 (2005).

- Staron, R.S., Leonardi, M.J., Karapondo, D.L., Malicky, E.S., Falkel, J.E., Hagerman, F.C., Hikida, R.S. Strength and Skeletal Muscle Adaptations in Heavy-Resistance-Trained Women After Detraining and Retraining. *Journal of Applied Physiology*. **70(2)**, 631-640 (1991).
- Stephens, J.A. and Usherwood, T.P. The Mechanical Properties of Human Motor Units with Special Reference to Their Fatiguability and Recruitment Threshold. *Brain Research*. **125(1)**, 91-97 (1977).
- Tidball, J.G. Mechanical Signal Transduction in Skeletal Muscle Growth and Adaptation. *Journal of Applied Physiology*. **98(5)**, 1900-1908 (2005).
- Van der Meer, S.F.T., Jaspers, R.T., Degens, H. Is the Myonuclear Domain Size Fixed? *Journal of Musculoskeletal and Neuronal Interactions*. **11(4)**, 286-297 (2011).
- Virgilio, K.M., Martin, K.S., Peirce, S.M., Blemker, S.S. Multiscale Models of Skeletal Muscle Reveal the Complex Effects of Muscular Dystrophy on Tissue Mechanics and Damage Susceptibility. *Interface Focus*. **5(2)**, (2015).
- Widrick, J.J., Romatowski, J.G., Bain, J.L.W., Trappe, S.W., Trappe, T.A., Thompson, J.L., Costill, D.L., Riley, D.A., Fitts, R.H. Effect of 17 Days of Bed Rest on Peak Isometric Force and Unloading Shortening Velocity of Human Soleus Fibers. *American Journal of Physiology Cell Physiology*. **273(5)**, C1690-C1699 (1997).
- Wisdom, K.M., Delp, S.L., Kuhl, E. Use It or Lose It: Multiscale Skeletal Muscle Adaptation to Mechanical Stimuli. *Biomechanics and Modeling in Mechanobiology*. **14(2)**, 195-215 (2015).

## 7 Appendix

### 7.1 Model Acronyms and Terms

ABM: Agent-based model.

Atrophy: Process by which muscle fibers decrease their size.

$\beta_d$ : Protein degradation rate coefficient  $\left[\frac{1}{\text{day}}\right]$ .

$\beta_s$ : Protein synthesis rate coefficient  $\left[\frac{\mu\text{m}^2}{\text{nuclei} \cdot \text{day}}\right]$ .

CSA: Cross-sectional area.

Fiber: Multinucleated, cellular unit of muscle tissue comprised of myofibrils.

Hypertrophy: Process by which muscle fibers increase their size.

MND: Myonuclear Domain. Finite volume of muscle fiber upkept by a single myonucleus.

Motor Unit: Functional unit of muscle comprised of an  $\alpha$ -motor neuron and all the fibers it enervates.

Muscle Memory: Muscle fibers retain a history of physical activity by retraining myonuclei during atrophy.

MVC: Maximum Voluntary Contraction.

Myofibril: Rod-like unit of muscle fiber comprised of sarcomeres added in series and in parallel.

Myonuclear Addition: The process by which Myonuclei are added to the fiber through fusion of Satellite Stem Cells.

Myonucleus: Nucleus of muscle fiber.

Nuclei: Model variable describing the number of effective myonuclei felt by the fiber cross-section.

PD: Protein deposition rate  $\left[\frac{\mu\text{m}^2}{\text{week}}\right]$ .

$\text{PD}_{\max}$ : Maximum protein deposition rate  $\left[\frac{\mu\text{m}^2}{\text{week}}\right]$ .

RE: Resistance Exercise.

## 7.2 Netlogo Code, Version 6.0.1

```

globals [totalfibers elapsed restperiod restcount
currentfiber MNcount MNmax]
breed [fibers fiber]
fibers-own [CSA fibertype activated goalCSA
fatigue myonuclei MND Bs Bd ]
patches-own []

to reset
  clear-all
  reset-ticks
  set-current-directory
  "F://BLEMKER_LAB/Thesis"
end

to setup
  reset
  ;ask patches [set pcolor 7] ; make background
  look like ECM
  set-default-shape fibers "circle"
  createfibers
  assignfibersizes
  set elapsed 0
  set restperiod Rest_Interval + 1
  set restcount restperiod ;begins with a
  workout
  set MNmax 4
end

to createfibers
  set totalfibers 0
  let spotx max-pxcor / 2
  let spoty max-pycor / 2
  ask patch spotx spoty [
    set totalfibers totalfibers + 1
    sprout-fibers 1
    [
      set size 6 set color red set CSA 200 set
  heading 90
    ]

  ]
  set totalfibers totalfibers + 1
  ; fiber count starts from 0
  ask fiber 0 [
    hatch-fibers 1 [set size 6 set color red set CSA
200]
  ]
  let fasciclesize Number_of_Fibers

```

```

  let grid 10 ; grid distance
  let steps 1 ; how many "steps" forward is the
  fiber going to make
  let counter 1 ; counts up to 2 sets of steps
  let dummy 0 ; counts steps fiber has made
  while [totalfibers < fasciclesize]
  [
    if dummy = steps
    [
      ask fiber 0 [rt 90]
      set dummy 0
      set counter counter + 1
    ]
    if counter > 2
    [
      set counter 1
      set steps steps + 1
      set dummy 0
    ]

    ask fiber 0
    [
      set dummy dummy + 1
      set totalfibers totalfibers + 1
      fd grid
      hatch-fibers 1
      [
        set size 6 set color red set CSA 200
      ]
    ]
  ]

  ask fiber 0 [fd grid]

  ; ask fibers [create-links-with other fibers in-
  radius 10]
  ; adjust

end

to assignfibersizes
  ask fibers ; will run this sequence for each
  fiber
  [
    ;assign fiber type
    let fibertypeprobability random-float 1

```



```

    ifelse fibertypeprobability < Percent_Type_I /
100 ;this gets all 3 fiber types
    [
        set fibertype 1 ;I
    ]
    [
        ifelse fibertypeprobability <
(Percent_Type_I + Percent_Type_IIA) / 100
        [
            set fibertype 2 ;IIA
        ]
        [
            set fibertype 3 ;IIB
        ]
    ]

; assign fiber colors
if fibertype = 3 [set color pink + 2]
if fibertype = 2 [set color magenta + 2]
if fibertype = 1 [set color red + 2]

; assign fiber CSA
let fiberCSA 0
if fibertype = 1
[
    set fiberCSA random-normal Type_I_mean
Type_I_std
    set CSA fiberCSA
    set size sqrt(CSA / dimension)
    set Bs Type_I_synth
    set Bd Type_I_degrad
]
if fibertype = 2
[
    set fiberCSA random-normal
Type_IIA_mean Type_IIA_std
    set CSA fiberCSA
    set size sqrt(CSA / dimension)
    set Bs Type_IIA_synth
    set Bd Type_IIA_degrad
]
if fibertype = 3
[
    set fiberCSA random-normal
Type_IIB_mean Type_IIB_std
    set CSA fiberCSA
    set size sqrt(CSA / dimension)
    set Bs Type_IIB_synth
    set Bd Type_IIB_degrad
]
]

```

```

ask fibers
[
    set myonuclei CSA / 2000
    set MND CSA / myonuclei
]

end

to setup_diameter
    reset
    ;ask patches [set pcolor 7] ; make background
look like ECM
    set-default-shape fibers "circle"
    createfibers
    assignfibersizes_diameter
    set elapsed 0
    set restperiod Rest_Interval + 1
    set restcount restperiod ;begins with a
workout
    set MNmax 4
end

to assignfibersizes_diameter
    ask fibers ; will run this sequence for each
fiber
    [
        ;assign fiber type
        let fibertypeprobability random-float 1
        ifelse fibertypeprobability < Percent_Type_I /
100 ;this gets all 3 fiber types
        [
            set fibertype 1 ;I
        ]
        [
            ifelse fibertypeprobability <
(Percent_Type_I + Percent_Type_IIA) / 100
            [
                set fibertype 2 ;IIA
            ]
            [
                set fibertype 3 ;IIB
            ]
        ]

; assign fiber colors
if fibertype = 3 [set color pink + 2]
if fibertype = 2 [set color magenta + 2]
if fibertype = 1 [set color red + 2]

; assign fiber CSA
let fiberCSA 0

```

```

let diameter 0
if fibertype = 1
[
  set diameter random-normal Type_I_mean
Type_I_std
  set fiberCSA pi / 4 * diameter ^ 2
  set CSA fiberCSA
  set size sqrt(CSA / dimension)
  set Bs Type_I_synth
  set Bd Type_I_degrad
]
if fibertype = 2
[
  set diameter random-normal
Type_IIA_mean Type_IIA_std
  set fiberCSA pi / 4 * diameter ^ 2
  set CSA fiberCSA
  set size sqrt(CSA / dimension)
  set Bs Type_IIA_synth
  set Bd Type_IIA_degrad
]
if fibertype = 3
[
  set diameter random-normal Type_IIB_mean
Type_IIB_std
  set fiberCSA pi / 4 * diameter ^ 2
  set CSA fiberCSA
  set size sqrt(CSA / dimension)
  set Bs Type_IIB_synth
  set Bd Type_IIB_degrad
]
]
ask fibers
[
  set myonuclei CSA / 2000
  set MND CSA / myonuclei
]
end

```

```

to myonucleiadapt
ask fibers
[
  if MND > 2000
  [
    set myonuclei CSA / 2000
    if myonuclei > MNmax [set myonuclei
MNmax]
  ]
  set MND CSA / myonuclei

```

```

]
end

.....
; Routine
.....
.....

to go
  set restperiod Rest_Interval + 1
  set restcount restcount + 1
  set MNcount MNcount + 1
  if not bed_rest?
  [
    daily_activity
    if exercise? and restcount >= restperiod
    [
      set restcount 0
      exercise
    ]
  ]

  rest      ; sleep
  fiberadapt
  if exercise? and MNcount >= 14
  [
    myonucleiadapt
    set MNcount 0
  ]
  ask fibers[set MND CSA / myonuclei]
  set elapsed elapsed + timestep
  if elapsed = timeframe
  [
    stop
  ]
  tick
end

```

```

to exercise
  recruitment
  Adapt_Protein_Balance
end

to recruitment
  ; recruitment thresholds according to tanji and
  kato
  let activation Percent_1RM
  let recruitmentprobability 0
  ask fibers with [fibertype = 1]

```

```

[
  let recruit random-float 1
  set recruitmentprobability 0.0096 * activation
+ 0.1458
  if recruitmentprobability < 0 [set
recruitmentprobability 0]
  if recruitmentprobability > 1 [set
recruitmentprobability 1]
  ifelse recruit < recruitmentprobability
  [
    set activated 1
    set color color - 1
    set fatigue fatigue + 1
  ]
  [set activated 0]
  if color < 10 [set color 10] ; sets fiber color to
black (all used up)
]

ask fibers with [fibertype = 2]
[
  let recruit random-float 1
  set recruitmentprobability 0.0106 * activation
+ 0.0543
  if recruitmentprobability < 0 [set
recruitmentprobability 0]
  if recruitmentprobability > 1 [set
recruitmentprobability 1]
  ifelse recruit < recruitmentprobability
  [
    set activated 1
    set color color - 1
    set fatigue fatigue + 1
  ]
  [set activated 0]
  if color < 120 [set color 120] ; sets fiber color
to black (all used up)
]

ask fibers with [fibertype = 3]
[
  let recruit random-float 1
  set recruitmentprobability 0.0125 * activation
- 0.109
  if recruitmentprobability < 0 [set
recruitmentprobability 0]
  if recruitmentprobability > 1 [set
recruitmentprobability 1]
  ifelse recruit < recruitmentprobability
  [
    set activated 1

```

```

    set color color - 1
    set fatigue fatigue + 1
  ]
  [set activated 0]
  if color < 130 [set color 130] ; sets fiber color
to black (all used up)
]

end

to Adapt_Protein_Balance
ask fibers with [activated = 1]
[
  if fibertype = 1
  [
    set Bs Bs + Bsinc * Bs ; protein synthesis
inc by Bsinc% [Biolo et al]
    set Bd Bd + Bdinc * Bd ; protein
degradation increase by Bdinc% [Biolo et al]
    if Bs > Type_I_Bsmax [set Bs
Type_I_Bsmax]
    if Bd > Type_I_Bdmax [set Bd
Type_I_Bdmax]
  ]

  if fibertype = 2
  [
    set Bs Bs + Bsinc * Bs ; protein synthesis
inc by Bsinc% [Biolo et al]
    set Bd Bd + Bdinc * Bd ; protein
degradation increase by Bdinc% [Biolo et al]
    if Bs > Type_IIA_Bsmax [set Bs
Type_IIA_Bsmax]
    if Bd > Type_IIA_Bdmax [set Bd
Type_IIA_Bdmax]
  ]

  if fibertype = 3
  [
    set Bs Bs + Bsinc * Bs ; protein synthesis
inc by Bsinc% [Biolo et al]
    set Bd Bd + Bdinc * Bd ; protein
degradation increase by Bdinc% [Biolo et al]
    if Bs > Type_IIB_Bsmax [set Bs
Type_IIB_Bsmax]
    if Bd > Type_IIB_Bdmax [set Bd
Type_IIB_Bdmax]
  ]
]

end

```

```

to fiberadapt
  ask fibers ;This will run sequence for each
  fiber individually
  [
    ; Initialize all values
    let currentCSA CSA

    ; assign new goal fiber CSA to each fiber.
    New total CSA is a simple equation of CSA
    breakdown + synthesis changing the current
    CSA content in a muscle
    set goalCSA currentCSA + Bs * myonuclei *
    timestep - Bd * currentCSA * timestep

    ; hypertrophy or atrophy by changing fiber
    CSA and size
    set CSA goalCSA
    set size sqrt(CSA / dimension)
  ]
end

to rest
  ; prescribe regenerative abilities of fibers per
  day

  ask fibers [
    set activated 0
    if fibertype = 1 and color < 17
    [set color color + 1]
    if fibertype = 2 and color < 127
    [set color color + 1]
    if fibertype = 3 and color < 137
    [set color color + 1]

    set fatigue 0
    if fibertype = 1
    [
      set Bs Bs - (Bs - Type_I_synth) / 3
      set Bd Bd - (Bd - Type_I_degrad) / 3
    ]
    if fibertype = 2
    [
      set Bs Bs - (Bs - Type_IIA_synth) / 3
      set Bd Bd - (Bd - Type_IIA_degrad) / 3
    ]
    if fibertype = 3
    [
      set Bs Bs - (Bs - Type_IIB_synth) / 3

```

```

      set Bd Bd - (Bd - Type_IIB_degrad) / 3
    ]
  ]

  ; make sure fiber color does not exceed healthy
  color and Bs does not fall below baseline value
  ask fibers with [fibertype = 1]
  [
    if color > 17 [set color 17]
    if Bs < Type_I_synth [set Bs Type_I_synth]
    if Bd < Type_I_degrad [set Bd
    Type_I_degrad]
  ]
  ask fibers with [fibertype = 2]
  [
    if color > 127 [set color 127]
    if Bs < Type_IIA_synth [set Bs
    Type_IIA_synth]
    if Bd < Type_IIA_degrad [set Bd
    Type_IIA_degrad]
  ]
  ask fibers with [fibertype = 3]
  [
    if color > 137 [set color 137]
    if Bs < Type_IIB_synth [set Bs
    Type_IIB_synth]
    if Bd < Type_IIB_degrad [set Bd
    Type_IIB_degrad]
  ]
end

to daily_activity
  ask fibers [
    if fibertype = 1 [
      set Bs Bs + 0.18 * Bs
      set Bd Bd + 0.06 * Bd
    ]
    if fibertype = 2 [
      set Bs Bs + 0.1 * Bs
      set Bd Bd + 0.06 * Bd
    ]
    if fibertype = 3 [
      set Bs Bs + 0.13 * Bs
      set Bd Bd + 0.05 * Bd
    ]
  ]
end

```